

NASA/TM—2007-214663



# Comparison of GRCop-84 to Other High Thermal Conductive Cu Alloys

*Henry C. de Groh III and David L. Ellis  
Glenn Research Center, Cleveland, Ohio*

*William S. Loewenthal  
Ohio Aerospace Institute, Brook Park, Ohio*

## NASA STI Program . . . in Profile

Since its founding, NASA has been dedicated to the advancement of aeronautics and space science. The NASA Scientific and Technical Information (STI) program plays a key part in helping NASA maintain this important role.

The NASA STI Program operates under the auspices of the Agency Chief Information Officer. It collects, organizes, provides for archiving, and disseminates NASA's STI. The NASA STI program provides access to the NASA Aeronautics and Space Database and its public interface, the NASA Technical Reports Server, thus providing one of the largest collections of aeronautical and space science STI in the world. Results are published in both non-NASA channels and by NASA in the NASA STI Report Series, which includes the following report types:

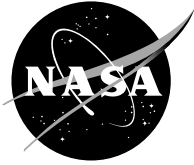
- **TECHNICAL PUBLICATION.** Reports of completed research or a major significant phase of research that present the results of NASA programs and include extensive data or theoretical analysis. Includes compilations of significant scientific and technical data and information deemed to be of continuing reference value. NASA counterpart of peer-reviewed formal professional papers but has less stringent limitations on manuscript length and extent of graphic presentations.
- **TECHNICAL MEMORANDUM.** Scientific and technical findings that are preliminary or of specialized interest, e.g., quick release reports, working papers, and bibliographies that contain minimal annotation. Does not contain extensive analysis.
- **CONTRACTOR REPORT.** Scientific and technical findings by NASA-sponsored contractors and grantees.

- **CONFERENCE PUBLICATION.** Collected papers from scientific and technical conferences, symposia, seminars, or other meetings sponsored or cosponsored by NASA.
- **SPECIAL PUBLICATION.** Scientific, technical, or historical information from NASA programs, projects, and missions, often concerned with subjects having substantial public interest.
- **TECHNICAL TRANSLATION.** English-language translations of foreign scientific and technical material pertinent to NASA's mission.

Specialized services also include creating custom thesauri, building customized databases, organizing and publishing research results.

For more information about the NASA STI program, see the following:

- Access the NASA STI program home page at <http://www.sti.nasa.gov>
- E-mail your question via the Internet to [help@sti.nasa.gov](mailto:help@sti.nasa.gov)
- Fax your question to the NASA STI Help Desk at 301-621-0134
- Telephone the NASA STI Help Desk at 301-621-0390
- Write to:  
NASA Center for AeroSpace Information (CASI)  
7115 Standard Drive  
Hanover, MD 21076-1320



# Comparison of GRCop-84 to Other High Thermal Conductive Cu Alloys

*Henry C. de Groh III and David L. Ellis  
Glenn Research Center, Cleveland, Ohio*

*William S. Loewenthal  
Ohio Aerospace Institute, Brook Park, Ohio*

National Aeronautics and  
Space Administration

Glenn Research Center  
Cleveland, Ohio 44135

## Acknowledgments

We would like to praise and acknowledge the dedicated support of our technicians and machine shop personnel: John Zoha, Sharon Thomas, Bill Armstrong, John Juhas, Adrienne Veverka, Ronald Phillips, Dave Brinkman, Aldo Panzanella, and Tim Ubienski; as well as our furnace/heat treat engineer Mark Jaster. Their support has enabled timely progress on this effort.

This report is a formal draft or working paper, intended to solicit comments and ideas from a technical peer group.

This report contains preliminary findings, subject to revision as analysis proceeds.

Trade names and trademarks are used in this report for identification only. Their usage does not constitute an official endorsement, either expressed or implied, by the National Aeronautics and Space Administration.

*Level of Review:* This material has been technically reviewed by technical management.

Available from

NASA Center for Aerospace Information  
7115 Standard Drive  
Hanover, MD 21076-1320

National Technical Information Service  
5285 Port Royal Road  
Springfield, VA 22161

Available electronically at <http://gltrs.grc.nasa.gov>

# Contents

Abstract.....	1
I. Introduction .....	1
II. Test Procedures .....	4
A. Tensile and Creep Procedures.....	4
B. Thermal Expansion Procedures.....	5
C. Strength Recovery Test for Cu-1Cr-0.1Zr .....	5
III. Test Results.....	6
A. Microstructures .....	6
B. Tensile and Compression Tests.....	7
C. Cooling Rate Effects on Hardenability of Cu-1Cr-0.1Zr.....	8
D. Creep Tests.....	8
E. Thermal Expansion.....	9
IV. Discussion.....	9
A. Comparison of Properties .....	9
B. Microstructure-Property Relations.....	10
C. Property Implications on Alloy Selection.....	10
D. Future Work .....	11
V. Summary and Conclusions.....	11
Tables.....	12
Table 1. Composition of Cu alloys in weight percent. ....	12
Table 2. Simulated braze heat treatment.....	12
Table 3. Ultimate Tensile Stress (UTS) in units of MPa for GRCo-84, AMZIRC, GlidCo Al-15, Cu-1Cr-0.1Zr, and Cu-0.9Cr alloys at various test temperatures; numbers in the table are averages of multiple tests, five tests at each temperature for GRCo-84, most others are the average of two tests. ....	13
Table 4. Yield Stress (YS) in units of MPa defined as the stress at 0.2% off-set strain, for GRCo-84, AMZIRC, GlidCo Al-15, Cu-1Cr-0.1Zr, and Cu-0.9Cr alloys at various test temperatures; numbers in the table are averages of multiple tests, five tests at each temperature for GRCo-84, most others are the average of two tests. ....	13
Table 5. Elongation, in units of %, defined as the change in gage length divided by the initial gage length times 100%, for GRCo-84, AMZIRC, GlidCo Al-15, and Cu-1Cr-0.1Zr alloys at various test temperatures; numbers in the table are averages of multiple tests, five tests at each temperature for GRCo-84, most others are the average of two tests. ....	14
Table 6. Reduction in area (R/A) in units %, defined as the change in cross-sectional area divided by the initial area times 100%, for GRCo-84, AMZIRC, GlidCo Al-15, and Cu-1Cr-0.1Zr alloys at various test temperatures; numbers in the table are averages of multiple tests, five tests at each temperature for GRCo-84, most others are the average of two tests. ....	14

Table 7. Compressive Yield Strength, in units MPa, defined as the compressive stress at 0.2% off-set strain, for GRCo-84, AMZIRC, GlidCo Al-15, Cu-1Cr-0.1Zr, and Cu-0.9Cr alloys at various test temperatures; numbers in the table are averages of multiple tests, two or three tests at each temperature for GRCo-84, all of the values for the other alloys are the average of two tests. ....	15
Table 8. Step Loaded, Creep Strain Rates at various temperatures, in units of strain/second, with 5 hours at each stress listed, for up to 20 steps, or failure. Creep, or strain rate, was defined as the slope of the time-strain data at the inflection point between primary and tertiary creep. ....	16
Table 9. Power function constants for step loaded, secondary steady state creep; creep rate power functions of the form $\dot{\epsilon} = A\sigma^n$ where $A$ and $n$ are given in the table, $\dot{\epsilon}$ is creep rate in units of $\text{sec}^{-1}$ , and $\sigma$ is step loaded creep stress in units of MPa. ....	20
Table 10. Constant load, steady state creep rate and creep life to failure; stress is initial stress based on initial cross sectional area. Creep, or strain rate, was defined as the slope of the time-strain data at the inflection point between primary and tertiary creep. ....	21
Table 11. Power function constants for constant load, secondary, steady state tensile creep at elevated temperatures; creep rate power functions of the form $\dot{\epsilon} = A\sigma^n$ where $A$ and $n$ are given in the table, $\dot{\epsilon}$ is creep rate in units of $\text{sec}^{-1}$ , and $\sigma$ is constant load creep stress in units of MPa. ....	25
Table 12. Thermal Expansion of AMZIRC, GlidCo Al-15, Cu-1Cr-0.1Zr, and Cu-0.9Cr alloys where the thermal expansion, $\alpha$ , in units of in/in, is expressed as a quadratic function of temperature, $T$ , in units of $^{\circ}\text{C}$ , such that $\alpha(T) = A(T)^2 + B(T) + C$ . Based on the variations of $\alpha$ expressed among different specimens, $\alpha$ values are estimated to be accurate to within $\pm 1\%$ . ....	25
Table 13. Summary and comparison of alloy properties. ....	26
Figures.....	27
Figure 1. Schematic of regeneratively cooled combustion chamber. (borrowed from Boeing and Ref. 1).....	27
Figure 2. Specimen designed used for AMZIRC tensile and creep specimens. ....	27
Figure 3. Tensile and creep specimen design used for GlidCo Al-15, Cu-0.9Cr, and Cu-1Cr-0.1Zn alloys. ....	28
Figure 4. Low-Cycle fatigue specimen designed used for all alloys tested in LCF; LCF results presented elsewhere.....	28
Figure 5. Typical as-extruded GRCo-84 microstructures.....	28
Figure 6. AMZIRC longitudinal microstructures in the as received condition; longitudinal/drawing direction is horizontal; dark spots are likely $\text{Cu}_5\text{Zr}$ .....	29
Figure 7. AMZIRC longitudinal microstructures after the simulated brazing heat treatment at $935^{\circ}\text{C}$ ; longitudinal/drawing direction is horizontal. ....	29
Figure 8. GlidCo Al-15 longitudinal micrograph of the as received condition; longitudinal/drawing direction is horizontal.....	29

Figure 9. GlidCop Al-15 longitudinal microstructures after the simulated brazing heat treatment at 935 °C; longitudinal/drawing direction is horizontal .....	30
Figure 10. Cu-1Cr-0.1Zr micrograph of the as received condition. ....	30
Figure 11. Cu-1Cr-0.1Zr longitudinal microstructures after the simulated brazing heat treatment at 935 °C; longitudinal/drawing direction is horizontal. ....	30
Figure 12. Cu-0.9Cr micrograph of the as received condition. ....	31
Figure 13. Cu-0.9Cr micrograph of the brazed condition.....	31
Figure 14. Ultimate tensile stress for as-received and brazed GRCop-84, AMZIRC, GlidCop Al-15, Cu-1Cr-0.1Zr, and Cu-0.9Cr alloys. GRCop-84 values are the average of HIPed and extruded material, data points represent averages of multiple tests, five tests at each temperature for GRCop-84, most others are the average of two tests.....	32
Figure 15. Yield Strength, in units of MPa, at 0.2% off-set strain for as-received and brazed GRCop-84, AMZIRC, GlidCop Al-15, Cu-1Cr-0.1Zr, and Cu-0.9Cr alloys. GRCop-84 values are the average of HIPed and extruded material, data points represent averages of multiple tests, five tests at each temperature for GRCop-84, most others are the average of two tests.....	32
Figure 16. Elongation in tensile of as-received and braze heat treated GRCop-84, AMZIRC, GlidCop Al-15, Cu-1Cr-0.1Zr, and Cu-0.9Cr alloys. Data points represent averages of multiple tests, five tests at each temperature for GRCop-84, most others are the average of two tests. ....	33
Figure 17. Reduction in cross-sectional area for as-received and brazed GRCop-84, AMZIRC, GlidCop Al-15, Cu-1Cr-0.1Zr, Cu-0.9Cr alloys. GRCop-84 values are the average of HIPed and extruded material, data points represent averages of multiple tests, five tests at each temperature for GRCop-84, most others are the average of two tests.....	33
Figure 18. Compressive Yield Strength, defined as the compressive stress at 0.2% off-set strain, for GRCop-84, AMZIRC, GlidCop Al-15, Cu-1Cr-0.1Zr, and Cu-0.9Cr alloys at various test temperatures; data points are from averages of multiple tests, two or three tests at each temperature for each alloy. ....	34
Figure 19. Stress-strain curve in tension at 500 °C for a) as received AMZIRC and b) AMZIRC which has received the simulated brazing heat treatment; note the drop in ultimate stress and rise in peak strain compared to as received AMZIRC...34	34
Figure 20. Stress-strain curve at 500 °C for GlidCop Al-15 in the a) as received condition, and b) after receiving the simulated braze heat treatment. ....	35
Figure 21. Hardness of a Cu-1Cr-0.1Zr bar after various treatments; cooling rate is the average cooling rate achieved during the quench from the solution temperature, 980 to 500 °C. As received and brazed conditions are shown for reference; Quenched bar is hardness after solution heat treatment at 980 °C and water quenching (cooling rates of >5 K/s) or air quenching (cooling rates <1 K/s). ....	35
Figure 22. Steady state secondary creep strain rates during step loading at 500 and 650 °C of a) GRCop-84; b) AMZIRC; c) GlidCop Al-15; d) Cu-1Cr-0.1Zr; and e) Cu-0.9Cr. Small data point markers are at 500 °C, larger symbols are at 650 °C;	

open data markers are as received, filled data points have received the simulated braze heat treatment at 935 °C.....	36
Figure 23. Step loaded creep rate data in the linear region of the log – log plot of strain rate and applied stress, with superimposed power function; power function constants are given in Table 9. All data at 500 °C are in black and use smaller symbols, data at 650 and 800 °C are gray (or color in the PDF version of this paper).....	37
Figure 24. Strain-Time data during step loaded creep at 500 °C for AMZIRC in the a) as received condition, and b) after receiving the simulated braze at 935 °C; the slopes of the steps are given in Table B6.....	38
Figure 25. Step loaded creep strain in time at 500 °C for GlidCop Al-15 in the a) as received condition, and b) after the simulated braze at 935 °C; the slopes of the steps are given in Table B6.....	38
Figure 26. Time to failure during constant tensile load at 500 and 650 °C for a) GRCop-84; b) AMZIRC; c) GlidCop Al-15; d) Cu-1Cr-0.1Zr; and e) Cu-0.9Cr. Small data point markers are at 500 °C, larger symbols are at 650 °C; open data markers are as received, filled data points have had the simulated braze heat treatment at 935 °C. The lines in a) are through creep life averages at each stress.....	39
Figure 27. Constant load creep and resulting secondary creep strain rates with superimposed power law functions, power function constants shown in Table 11; data at 500 °C are black, larger like symbols are at the higher temperature. The GRCop-84 lines shown are from the power law creep rate equations presented in Table 11, from analysis of previous creep tests presented in Ref. 21.....	40
Figure 28. Constant load creep at 500 °C for AMZIRC in the a) as received condition, initial stress = 87 MPa, resulting in a creep rate of $3.8 \times 10^{-8}$ /sec, and b) after the simulated braze, initial stress = 60 MPa, resulting in a creep rate of $2.3 \times 10^{-6}$ /sec....	40
Figure 29. Constant load creep at 650 °C of as received Amzirc with initial stress = 15 MPa, resulting in a creep rate of $3.7 \times 10^{-6}$ /sec.....	41
Figure 30. Constant load creep of GRCop-84 at 500 °C at an initial stress of 84 MPa, resulting in a creep rate of $7.31 \times 10^{-8}$ /sec. ....	41
Figure 31. Thermal Expansion results, lines are plots of equation (1) and the quadratics from Table 12.....	41
References.....	42



# Comparison of GRCop-84 to Other High Thermal Conductive Cu Alloys

Henry C. de Groh III and David L. Ellis  
National Aeronautics and Space Administration  
Glenn Research Center  
Cleveland, Ohio 44135

William S. Loewenthal  
Ohio Aerospace Institute  
Brook Park, Ohio 44142

## Abstract

The mechanical properties of five copper alloys with high thermal conductivity, GRCop-84, AMZIRC, GlidCop Al-15, Cu-1Cr-0.1Zr, and Cu-0.9Cr were compared. These are competing alloys in high temperature, high heat flux applications such as rocket nozzles. The GRCop-84 data presented was taken from previous work. The results of new tensile, creep, thermal expansion, and compression tests on AMZIRC, GlidCop Al-15, Cu-1Cr-0.1Zr, and Cu-0.9Cr are presented. Tests were done on as-received hard drawn material, and on material that had been subjected to a heat treatment designed to simulate a brazing operation at 935 °C. In the as-received condition AMZIRC, GlidCop Al-15, Cu-1Cr-0.1Zr and Cu-0.9Cr had excellent tensile and compressive strengths at temperatures below 500 °C. However, the simulated brazing heat treatment substantially decreased the mechanical properties of the precipitation strengthened AMZIRC, Cu-1Cr-0.1Zr, and Cu-0.9Cr, and the strength of as-received AMZIRC dropped precipitously as test temperatures exceeded 500 °C. The properties of the dispersion strengthened GlidCop Al-15 and GRCop-84 were not significantly affected by the 935 °C heat treatment. As a result, there appear to be advantages to GRCop-84 over AMZIRC, Cu-1Cr-0.1Zr, and Cu-0.9Cr if use or processing temperatures of greater than 500 °C are expected. Ductility was lowest in GlidCop Al-15 and Cu-0.9Cr; reduction in area was particularly low in GlidCop Al-15 above 500 °C, and as received Cu-0.9Cr was brittle between 500 and 650 °C. Tensile creep tests were done at 500 and 650 °C. At these temperatures, the creep properties of GRCop-84 were superior to those of brazed AMZIRC, Cu-1Cr-0.1Zr, and Cu-0.9Cr. The creep properties of Cu-0.9Cr were the worst. At equivalent rupture life and stress, GRCop-84 was found to have a 150 °C temperature advantage over brazed AMZIRC; for equivalent rupture life and temperature GRCop-84 was two times stronger. GlidCop Al-15 had the lowest creep rates at 500 and 650 °C. The advantages of GRCop-84 over GlidCop Al-15 associated with ease of processing were confirmed by GlidCop's marginal ductility. In the post brazed condition, GRCop-84 was found to be superior to the other alloys due to its greater strength and creep resistance (compared to AMZIRC, Cu-1Cr-0.1Zr, and Cu-0.9Cr) and ductility (compared to GlidCop Al-15).

## I. Introduction

GRCop-84 (Cu-8 at%Cr-4 at% Nb) is a newly-developed copper alloy with an attractive balance of high temperature strength, creep resistance, low cycle fatigue life, and thermal conductivity. This report will detail efforts at NASA Glenn to compare GRCop-84 to similar commercial copper alloys in a consistent manner. Data on alloys such as NARloy-Z, AMZIRC,

GlidCop Al-15 low oxygen grade, Cu-0.9Cr, and Cu-1Cr-0.1Zr can be found in the literature [1-13]. However, the test conditions are rarely matching for “apples-to-apples” comparisons. Most literature also deals only with as-received material. The alloys being considered in this work are used in high temperature applications where high thermal conductivity, high strength, and resistance to creep and low cycle fatigue are required. Such applications include high performance metal gaskets, rocket engine combustion chambers, nozzle liners, and various Reusable Launch Vehicle (RLV) technologies [1]. Figure 1 shows a schematic of a combustion chamber wherein these copper alloys might be used, particularly in the chamber liner and injector face plate. These parts are subjected to the combustion gas temperatures on the hot side and are cooled by cryogenic hydrogen flow on the back side. The tensile, creep, low cycle fatigue, and compressive strength of GRCop-84 will be compared to those of the existing commercially available alloys shown in Table 1. To compare the properties these alloys would actually have during use, they were tested in the as-received condition and after a heat treatment designed to simulate a typical high temperature brazing cycle often needed in the manufacturing process [2]. The selected brazing heat treatment cycle is presented in Table 2.

GRCop-84 is a dispersion and precipitation hardened alloy made using rapid solidification and powder metallurgical techniques. Consolidation is accomplished by hot isostatic pressing (HIP) or direct extrusion. After consolidation most processing methods used with high strength copper alloys can be used to form GRCop-84, e.g., hot and cold rolling. The solubilities of Cr and Nb are very high in liquid copper but very low in solid Cu. Chromium and Nb have a high affinity for each other, thus nearly all of the Cr and Nb combine to form the hardening intermetallic phase  $\text{Cr}_2\text{Nb}$ . This leaves a nearly pure Cu matrix. The high purity of the copper matrix leads to a thermal conductivity for the alloy that is 72% to 82% of that of pure oxygen-free Cu [3].

AMZIRC can be cast as well as produced using powder metallurgy. Peak strengths in AMZIRC are achieved through cold work combined with precipitation hardening and are lost if the hardened material is exposed to a high temperature braze cycle or if fully annealed [4]. Approximately 80% of the strength gains normally achieved in AMZIRC are due to cold work, with only modest additional gains achieved upon aging [5]. Horn and Lewis found that cold-worked AMZIRC retains much of its strength up to about 500 °C (932 °F) without becoming brittle. They also noted that the excellent strength of heavily worked rod was not achieved in their billets and that there was an inability to obtain uniform hardening in large billets [6]. AMZIRC’s low cycle fatigue properties have been reported by Conway et al. [7] and by Hannum et al. [8], and property reviews which have included AMZIRC have been published [5,9]. Dalder et al. found the room temperature ultimate tensile strength of AMZIRC to be about 430 MPa [10] and that AMZIRC’s room temperature strength dropped to 241 MPa after exposure to >500 °C. The room temperature ductility of AMZIRC decreases with cold work, with elongation at failure going from about 50% for unworked material to 10% [5] or lower [10] for material worked >30%. AMZIRC has a solution temperature near 910 °C (1670 °F) and aging temperatures near 525 °C (968 °F) for unworked material, and 425 °C (797 °F) for cold worked material.

GlidCop Al-15 is dispersion hardened with very fine  $\text{Al}_2\text{O}_3$  particles. Considerable research has been published on GlidCop Al-15. Dalder et al. [10] found GlidCop more thermally stable than AMZIRC. Wycliffe [5] found (in 1984) that the only copper alloys with good strength above 650 °C (1200 °F) were oxide dispersion strengthened (ODS) alloys such as GlidCop. However, Wycliffe also noted that the ductility and low cycle fatigue properties of

ODS copper alloys at elevated temperatures were poor. Stephens and Schmale showed that heat treat cycles which simulate brazing operations as high as 980 °C (1796 °F) result in only a small decline in ultimate tensile strength (~13%) in GlidCop Al-15, and that ductility improves substantially [2]. Stephens et al. [11] showed that fine-grained GlidCop Al-15 that was annealed for 15 minutes at 980 °C was stronger in room temperature tension than coarse-grained GlidCop Al-15 annealed 100 hr at 980 °C, but that as the test temperature increased, the advantage fine-grained GlidCop Al-15 had vanished, until at 800 °C (1472 °F) coarse-grained GlidCop Al-15 was stronger than fine-grained GlidCop Al-15. In work due to Conway et al. the ductility and low-cycle-fatigue properties of GlidCop were found to be low; however, the alloy tested is noted as GlidCop Al-10, which contains 0.2 wt.% Al<sub>2</sub>O<sub>3</sub> [4] versus 0.32 wt.% Al<sub>2</sub>O<sub>3</sub> for GlidCop Al-15.

Cu-0.9Cr is precipitation strengthened by elemental Cr precipitates and is known for excellent cold workability. Precipitation hardening for these alloys consists of solution treatments near 990 °C (1814 °F) for about 20 minutes, water quenching, and aging near 460 °C (860 °F) for about 3 hours [12]. Near peak strength in Cu-0.9Cr alloys is sometimes achieved during processing, due either to cold work, or precipitation hardening at process temperatures. In such cases only moderate gains in strength are possible with aging heat treatments [13]. The ductility of these alloys near the expected use temperatures of 400 to 600 °C (752 to 1112 °F) has been found to be poor compared to other copper alloys [5,6]. Room temperature strength in Cu-0.9Cr alloys is good, with UTS values near 500 MPa [4,5,6]. Strength declines with increasing temperature, particularly steeply as 427 °C (800 °F) is exceeded, with UTS values near 65 MPa at 593 °C (1100 °F) [5,6].

Cu-1Cr-0.1Zr is age hardenable, with Cr and Cu<sub>5</sub>Zr precipitates [14]. Pratt & Whitney presented work on an alloy, Cu-1Cr-0.5Zr, which was found to be very strong, but to have poor low cycle fatigue at 705 °C (1300 °F) compared to NARloy-Z and a Cu-0.47wt% Zr alloy (which is close to the composition of AMZIRC) [15]. The literature data indicates that at 538 °C (1000 °F), on the basis of total axial strain range versus number of cycles to failure, the fatigue properties of AMZIRC, and Cu-Zr alloys are better than those of Cu-Cr, NARloy-Z, and GlidCop Al-10 [4,5,7]. Ultimate and yield strengths at 705 °C for as-received material were approximately 175 and 94 MPa respectively. Tensile properties for Cu-Cr-Zr alloys are also reported by Zinkle [16]. The solution and aging temperatures for Cu-1Cr-0.1Zr are expected to be similar to AMZIRC and Cu-0.9Cr. The solution and aging temperatures for Cu-0.9Cr are approximately 990 °C (1814 °F) and 440 °C (824 °F) respectively. It has been proposed that strength lost in a precipitation strengthened Cu alloy liner during the brazing step of production might be regained through a post braze heat treatment to age harden the alloy [17]. Observations made by Pratt & Whitney on such heat treatments with Cu-1Cr-0.47Zr (wt.%) are thus worth noting here [15]. Some key observations are:

- 1) Peak hardness of about DPH 143 was achieved in two ways: a) through cold-working the as received extruded material, and b) by cold working and aging at 480 °C (896 °F) solutioned material.

- 2) Subsequent annealing at 650 °C (1202 °F) softened the cold-worked extruded material to DPH 110 *but did not* cause recrystallization. Subsequent annealing at 650 °C also softened (to DPH 72) the solutioned and cold-worked material – but in this case also caused recrystallization. Solutioning effectively lowered the energy barriers to

recrystallization, exacerbating the detrimental effects of the 650 °C anneal. Solution temperatures for the copper alloys we are considering are similar to nozzle brazing temperatures (935 to 990 °C).

3) Solutionizing the as-extruded material caused recrystallization and hardness to drop to DPH 70. Aging at 480 °C regained some of the lost hardness (DPH 100). Additional annealing at 650 °C caused over aging and softening to DPH 65.

The effectiveness of aging also depends on quench rates from solution temperatures. Relations between quench rates and hardenability in the Cu-1Cr-0.1Zr alloy were also examined as part of this work.

## II. Test Procedures

The test plan included tensile, compressive, creep, thermal expansion and low-cycle fatigue properties of all the alloys. Low-cycle fatigue results will be presented elsewhere. Detailed testing procedures have been presented previously [18,19,20] and will be only briefly outlined here.

All alloys were tested in both the as-received condition and after a simulated braze treatment. GRCop-84 was tested in two as-received conditions: as-extruded, and as-HIPed. AMZIRC, GlidCop Al-15, Cu-1Cr-0.1Zr, and Cu-0.9Cr alloys were received in the form of hard drawn rods that were 3/8 to 3/4 inch diameter. Table 2 shows the simulated braze cycle designated “Braze 935” which is meant to be typical of a main combustion chamber liner/jacket brazing operation. In addition, two Cu-1Cr-0.1Zr bars were heat treated to try to recover strength following the braze cycle.

### A. Tensile and Creep Procedures

Tensile and compression tests were conducted at 25, 200, 500, 650, and 800 °C (77, 392, 932, 1202 and 1472 °F) using strain rate control. Tests at elevated temperatures employed flowing Ar at 2.5 l/min. A strain rate of 0.005 mm/mm/min ( $8.3 \times 10^{-5} \text{ sec}^{-1}$ ) was used in both tensile and compression tests. Strain was measured via an extensometer attached to the gage of the tensile samples, but compression tests relied on crosshead displacement. Specimen designs used for tensile, creep, and low cycle fatigue are shown in Figures 2, 3, and 4. Compression specimens were cylinders 5.0 mm (0.197 in) in diameter by 10 mm (0.394 in) long.

Creep tests were done in vacuum at 500, 650, and 800 °C (932, 1202, and 1472 °F) using constant load lever arm vacuum creep units. The stresses in the creep tests were varied to give lives equivalent to 100 Space Shuttle missions (15 hours). For GRCop-84 creep stresses were about 100 MPa at 500 °C, 40 MPa at 650 °C, and 20 MPa at 800 °C. Stress levels for the other alloys typically had to be lower to achieve lives near 15 hours.

Creep testing of all alloys except GRCop-84 started with step loading vacuum creep tests using a converted Instron tensile test load frame. The load was held constant for five hours, and then raised a set amount every five hours for a total of 20 steps, or until failure. All creep tests were performed with at least two thermocouples attached to the ends of the gage area. For these creep tests, strain was measured by monitoring crosshead movement. All creep rates were defined as the slope of the linear portion of the creep strain-time curve between primary and tertiary creep.

In an effort to include previous constant load GRCop-84 creep tests, we have statistically modified some older GRCop-84 data to make it consistent with the methods used in this study. These data were then used to determine power law creep coefficients for comparison to the other alloys (see Table 11). The details of the statistical processing are in reference 21. These creep rate equations for GRCop-84 were plotted with the constant load creep data in Figure 27.

### **B. Thermal Expansion Procedures**

Thermal expansion of the candidate alloys was conducted using an Anter Unitherm 1161AL-V vertical two head pushrod dilatometer. Data acquisition was accomplished using proprietary hardware and software. Resolution of the displacement was 0.001 mm. A sample was loaded along with a Pt standard, and the chamber sealed. The chamber was evacuated and purged with argon several times to remove the oxygen from the chamber. During the final purge the pressure was reduced to  $\leq 39$  Pa (300 millitorr) prior to backfilling with Ar. Ar was selected over He based upon the tendency of Ar to collect at the bottom of the chamber and displace any residual oxygen in the vicinity of the sample.

The samples were heated to 1000 °C (1832 °F) using a heating rate of 3 °C (5.4 °F) per minute and then cooled to room temperature while the changes in length for both the copper alloy sample and Pt standard were measured. During cooling the rate was 3 °C per minute until the temperature reached approximately 175 °C (347 °F). At that point the samples underwent free cooling. Ar was flowing through the chamber during the test at a rate of approximately 50 cc per minute. This maintained the chamber at a slight positive pressure. Oxidation of the samples was minimal and did not affect the results. Each sample was given five cycles. Two samples of each alloy were tested.

During the test the displacement and temperature for both samples were measured simultaneously. Using the sample temperature and reference data for the thermal expansion of Pt [22], the actual displacement from the Pt sample's thermal expansion could be calculated for each data point. Subtracting this value from the measured displacement of the Pt sample allowed the calculation of the contribution of the thermal expansion of the alumina push rod and sample holder to the observed displacements. The contribution of the holder and push rod was then subtracted from the measured copper alloy displacement to calculate the actual thermal expansion of the Cu alloy sample at each data point. To calculate the thermal expansion strain, the displacement was divided by the original sample length. The data was then plotted and fitted with a second order polynomial equation. The thermal expansion of each specimen was measured five times, the results of these five cycles were averaged, and then the results of two specimens were averaged to yield the final empirical relations between thermal expansion and temperature.

### **C. Strength Recovery Test for Cu-1Cr-0.1Zr**

The hardness of two as received bars of Cu-1Cr0.1Zr was measured. Radial holes were drilled in these bars so that Type K thermocouples could be snugly inserted, with their tips bottoming out at the center of the bars, and spaced 2 cm apart along the length. A nickel powder-oil paste was put in the holes to improve contact between the Cu bar and thermocouples. These 1.59 cm (0.625 inch) diameter bars, 20.3 cm (8 inches), and 14.29 cm (5.625 inches) long, were then thoroughly insulated, except for one end, which was left exposed. These bars were then solution heat treated at 980 °C for 20 min.; after which the exposed end of the longer bar was quenched into ice water, and the end of the shorter bar air quenched using a fan. The

temperatures were monitored and each thermocouple reading recorded once per second. Cooling rates were not constant, so average cooling rates were determined by calculating the cooling rate every 26 seconds, and then averaging all of the measured cooling rates between 980 and 500 °C (1796 and 932 °F).

The hardness along the length of the quenched bars was measured. Since the hardness of hard drawn as received material and that of annealed Cu-1Cr-0.1Zr varies greatly, hardness was measured on either the Rockwell B scale or F scale and converted to the Rockwell Superficial 30-T scale using a table provided by Wilson.[23] All hardness measurements were made on cylindrical bars, which characteristically result in slightly lower hardness readings. All hardness readings were corrected using Wilson's cylindrical correction chart.[23]

Finally, both of these bars were age hardened for 1 hour at 500 °C. The hardness along their lengths was measured again. The water quenched bar was age hardened for another hour at 500 °C, and the hardness measured afterwards.

### III. Test Results

#### A. Microstructures

Figure 5 shows typical as-extruded GRCop-84 microstructure. The as-HIPed and brazed microstructures are visually indistinguishable from the as-extruded microstructure. GRCop-84 gains most of its added strength over pure copper from finely dispersed Cr<sub>2</sub>Nb precipitates such as those shown in Figure 5. The stability and melting point of Cr<sub>2</sub>Nb is so high that it begins to precipitate in the molten GRCop-84 before the onset of primary Cu solidification.[24] These stable Cr<sub>2</sub>Nb precipitates do not significantly coarsen during the brazing heat treatment or during use at high temperatures.

Figures 6 and 7 show the as-received and post brazed microstructures for AMZIRC. In Figure 7 it can be seen that the fine, elongated grain structure observed in as-received hard drawn AMZIRC (Figure 6) has given way to a much coarser structure of equiaxed grains with some twinning indicative of complete recrystallisation and considerable grain growth. The observed twinning is common for FCC metals during recrystallisation [25]. Rather large (~ 5 μm) precipitates are present in both as-received and brazed structures. These precipitates are believed to be high temperature Cu<sub>5</sub>Zr intermetallics formed during casting and not solutionized at the brazing temperature or at the solution temperatures normally used for AMZIRC (980 °C (1796 °F)).

The recrystallized grains in the brazed AMZIRC are essentially strain free. This lower dislocation density contributes to the decline in strength upon brazing as does the larger grain size through a Hall-Petch relationship [25].

Figures 8 and 9 show the as received and post brazed microstructures of GlidCop Al-15. As was the case for GRCop-84, the microstructure of GlidCop appears to be unaffected by the simulated braze heat treatment.

Figures 10 and 11 show the microstructures of as-received and post brazed Cu-1Cr-0.1Zr. The as received Cu-1Cr-0.1Zr has a fine grain structure, elongated along the drawing direction. The brazed material has recrystallized; but the grain size appears to have remained small, maybe even decreased compared to the as received Cu-1Cr-0.1 material. Thus the presence of Cr in the alloy prevented the extensive grain growth observed in AMZIRC after recrystallisation. What we

believe to be Cr and Cu<sub>5</sub>Zr precipitates can be seen in the high magnification micrographs (Figures 10 b), and 11 b)). The Cu<sub>5</sub>Zr precipitates, which have a melting point near 1030 °C (1886 °F), have an alignment due to the drawing process; since this alignment persists in the brazed microstructure it is concluded that the Cu<sub>5</sub>Zr precipitates are not solutionized at the 935 °C (1715 °F) brazing temperature, which is consistent with the ternary Cu-Cr-Zr phase diagram of Zeng et al. [14].

The Cu-0.9Cr structures shown in Figures 12 and 13 appear nearly identical to those seen in Cu-1Cr-0.1Zr, with the structure of the Cu-0.9Cr alloy consisting of fine, slightly elongated grains and Cr precipitates in the as received microstructures. The braze appears to have caused recrystallization (Figure 13) but extensive grain growth did not occur, as it did in the case of AMZIRC. The aligned precipitates in the as received structure (Figure 12 b) appear much more spherical after brazing (Figure 13 b).

## **B. Tensile and Compression Tests**

Room and elevated temperature tensile and compressive properties for the alloys are presented in Figures 14 through 20, and in Tables 3 through 7. In Figures 14 through 17, data points shown for GRCop-84 are from an average of five tests. Data points for AMZIRC are from the average of two tests except at the temperatures of 400, 500, 600 and 650 °C (752, 932, 1112, 1202 °F) which were single tests (see Tables 3-7). The data points for GlidCop Al-15, Cu-1Cr-0.1Zr, and Cu-0.9Cr were from the average of two tests. The compression data shown in Figure 18 were averaged from two or three tests.

The ultimate and yield strengths shown in Figures 14 and 15 indicate that in the as-received condition the competing alloys, AMZIRC, GlidCop, Cu-1Cr-0.1Zr, and Cu-0.9Cr are generally stronger than GRCop-84. However, after the simulated brazing heat treatment, the strength of AMZIRC, Cu-1Cr-0.1Zr and Cu-0.9Cr drop dramatically to strength levels significantly below GRCop-84. GlidCop Al-15 retains most of its strength after the brazing heat treatment making it stronger than GRCop-84 in tensile tests at all temperatures and conditions examined. There is an abrupt drop in the strength of as-received AMZIRC near 500 °C which appears to coincide with the onset of annealing and recrystallisation. The strength of Cu-1Cr-0.1Zr and Cu-0.9Cr drop more gradually as test temperatures are increased compared to AMZIRC. The trends apparent in the tensile strengths of the alloys are mirrored in compression as shown in Figure 18. Figures 19 and 20 provide examples of stress-strain curves at 500 °C for AMZIRC and GlidCop Al-15, in the brazed and as received conditions.

All failures were ductile except those for Cu-0.9Cr at temperatures between 500 and 650 °C. At these temperatures the ductility of Cu-0.9Cr was the lowest of all the alloys, with elongation and reduction in area being approximately 2% and 6.7% respectively. Exposing as-received AMZIRC to temperatures above 500 °C (932 °F) approximately tripled elongation, resulting in the highest elongations of any of the alloys (Figure 4). GRCop-84 and GlidCop Al-15 had approximately the same elongation. In general, it was found that as the testing temperature increased, uniform elongation increased and localized necking decreased which decreased the reduction in area measurements (R/A) as shown in Figure 17. At temperatures above 500 °C reduction in area was higher for GRCop-84 compared to GlidCop Al-15.

### C. Cooling Rate Effects on Hardenability of Cu-1Cr-0.1Zr

Figure 21 shows the hardness of Cu-1Cr-0.1Zr cooled at different rates after being solutioned at 980 °C (1796 °F). The peak hardness for Cu-1Cr-0.1Zr of about 75 HR30-T was observed in the as received material; the hardness in the as received and brazed conditions is shown on Figure 21 for reference. Hardness dropped dramatically to 12 HR30-T after the simulated braze heat treatment at 935 °C, and after solutioning and quenching to about 8 HR30-T. At cooling rates above 5 K/s from the solution temperature, the 1 hour age hardening heat treatment was enough to achieve substantial recovery in hardness (to about 57 HR30-T). The second hour of precipitation heat treatment overaged the material resulting in a drop in hardness. The ability of Cu-1Cr-0.1Zr to be age hardened drops precipitously as cooling rate from the solution temperature drops below 1 K/s. After age hardening, Cu-1Cr-0.1Zr cooled at 0.74 K/s had a hardness of about 20 HR30-T. Thus only about 15% of the hardness lost was recovered, versus 71% recovery for material with a cooling rate >5 K/s.

### D. Creep Tests

Results of step loading creep tests are shown in Figures 22 through 25 and Tables 8 and 9. Constant load creep results are shown in Figures 26 through 30 and Tables 10 and 11. All creep rates, or strain rates measured during creep tests, were defined as the linear portion of the time – strain data after load up and primary creep but before tertiary creep.

It can be seen in Figure 23 (and Table 8) that at a given stress at 500 °C (932 °F) the steady-state creep rate of as-received AMZIRC is about double that of GRCop-84, and the strain rate of brazed AMZIRC is about two orders of magnitude greater than GRCop-84. Similarly, strain rates of AMZIRC at 650 °C (1202 °F) at a stress of 20 MPa are about two orders of magnitude greater than the strain rates observed for GRCop-84 at 650 °C and 20 MPa.

From our experience, a creep rate of about  $5 \times 10^{-6} \text{ sec}^{-1}$  often yields a creep rupture life of about 15 hours assuming most of the creep life is spent in second stage or steady-state creep. Step loaded and constant load creep tests indicate that at 500 °C stresses of about 65 MPa and 130 MPa applied to brazed AMZIRC and GRCop-84 respectively are expected to yield approximately, 15 hour lives (Figures 23 and 27). Thus for equivalent temperatures and lives, GRCop-84 can sustain about double the creep stress compared to brazed AMZIRC. Note how close together the GRCop-84 (650 °C) and brazed AMZIRC (500 °C) curves are in Figure 23. This indicates that at equivalent stress and strain rate, such as  $\sigma = 47 \text{ MPa}$  and  $\dot{\epsilon} = 10^{-6} \text{ sec}^{-1}$ , GRCop-84 can operate at temperatures 150 °C (302 °F) higher than AMZIRC. GlidCop Al-15 performed very well, with creep rates much lower (at a given stress) than any of the other alloys at 500 °C. As received Cu-1Cr-0.1Zr also performed very well in creep, however, upon brazing creep properties declined substantially.

Often creep can be described by a rate equation of the form  $\dot{\epsilon} = A\sigma^n$ , where  $\dot{\epsilon}$  is creep strain rate,  $A$  is a constant,  $\sigma$  is creep stress, and  $n$  is the stress exponent. The power law creep constants for the step loaded creep tests and those resulting from the constant load creep tests were independently determined and are presented in Tables 9 and 11. The stress exponent  $n$  can help to identify creep mechanisms,[26] for example, dispersion strengthened materials commonly have high stress exponents, of the order of 20 to 100 due to the added resistance to dislocation glide caused by the particles. Before such an exploration of creep mechanisms, trends in our data, and areas where more data are needed will be examined. The creep stress exponents



$n$  for GRCop-84 at 500, 650 and 800 °C were fairly consistent, equal to about 9.5 in the step loaded creep tests, and 8 for constant load creep [21]. The stress exponents for GlidCop ranged from 12.4 to 91.2 (see Tables 9 and 11) and the exponents resulting from step loaded creep (Table 9) were consistently and significantly lower than the exponents resulting from constant load creep (Table 11). The stress exponents for AMZIRC averaged about 5.3 (with a range of 2.35 to 9.49),  $n$  averaged about 5.1 for the Cu-1Cr-0.1Zr creep tests, and the average stress exponent for the Cu-0.9Cr tests was 4.4.

### E. Thermal Expansion

Thermal expansion results are presented in Figure 31 and Table 12. Figure 31 shows plots of the equations presented in Table 12. The best fit equation for GRCop-84 with two-way confidence intervals taken from reference [27] is:

$$\alpha(T) = (-0.3287 + 2.265 \times 10^{-4} T^{1.285}) \pm t(1 - \frac{\alpha}{2}, 10) \sqrt{(1.403 \times 10^{-2})^2 + (2.038 \times 10^{-5} T)^2} \quad (1)$$

where T is in Kelvin,  $t(1-\alpha/2, 10)$  is the value for the t-distribution with 10 degrees of freedom associated with  $1-\alpha/2$  cumulative probability, and  $\alpha(T)$  is the thermal expansion of GRCop-84 in percent ( $\alpha(T)/100\%$  is plotted in Figure 31). The four alloys being compared to GRCop-84 have about the same thermal expansion. This is expected since they are all near 99% Cu. GRCop-84 however has about 14 vol.% Cr<sub>2</sub>Nb which retards temperature driven strains, and results in thermal expansion being between 7% and 15% lower for GRCop-84 than the other alloys at typical liner hot wall temperatures.

## IV. Discussion

### A. Comparison of Properties

Desirable properties for copper alloys being developed for rocket engine components include: low thermal expansion; high strength; high ductility; ease of processing; low creep rate; high compressive strength; high low-cycle-fatigue strength; high maximum operating temperature; and a minimum affect caused by component manufacture such as brazing. The data presented in this paper and the literature were considered in the comparison of GRCop-84 to the other alloys. A summary of this comparison is presented in Table 13.

High temperature creep in alloys involves the interaction of the stress fields of moving dislocations with those of stationary dislocations and other boundaries such as second phase particles and grain boundaries. Specific values of the stress exponent  $n$  are associated with particular creep mechanisms. Alloys that exhibit pure metal (or “class M”) behavior are characterized by  $n = 4$  to 8; exponent values in this range can be taken as evidence that the creep mechanism is dominated by dislocation climb. A majority of the creep data indicates that AMZIRC, Cu-0.9Cr, and Cu-1Cr-0.1Zr have stress exponents in this range, indicating dislocation climb, or class M, creep.

In some alloys solute atom clusters interact with dislocations and viscous glide of dislocations is the rate controlling process. The stress exponent for these “class A” (for alloy) materials is typically near 3. None of the alloys provided consistent stress exponents in this range.

Due to added interactions between dislocations and fine particles, dispersion strengthened materials usually have stress exponents of the order of 20 to 100. This enhanced sensitivity to

stress is believed to be due to the added energy required for dislocations to climb out of their glide planes to overcome the particles and the thermally activated release of those dislocations from the departure side of the particles [26]. GlidCop Al-15 had  $n$  values between 12 and 91, which are considered to be characteristic of dispersion strengthened alloys. Though data was limited, GRCop-84 had stress exponents in the range of 7.3 to 10, implying class M creep behavior (dislocation climb) with some added stress sensitivity resulting from the relatively large volume fraction of precipitates and grain boundaries.

Refer to Table 13 for comparisons of thermal conductivity and expansion, tensile and compressive strength, ductility, creep, and the effects of brazing on the alloys.

### **B. Microstructure-Property Relations**

Microstructures are shown in Figures 5 through 13. The large number of  $\text{Cr}_2\text{Nb}$  precipitates present in GRCop-84 (Figure 5) result in good strength, and since the precipitates are stable and do not significantly coarsen, properties decline moderately with increasing temperature. The same can be said for GlidCop Al-15 (Figures 8 and 9) microstructurally, though the precipitate is alumina. The microstructural feature that dominates properties in GRCop-84 and GlidCop is the stable precipitates. These precipitates enabled GRCop-84 and GlidCop to perform significantly better than the precipitation strengthened alloys in the brazed condition in both strength and creep.

By contrast, the microstructure of AMZIRC is dominated by the fine elongated grain boundaries and the benefits of work hardening (Figures 6 and 7). Though the as received microstructures of Cu-1Cr-0.1Zr and Cu-0.9Cr had some grain texturing characteristic of longitudinally drawn material, this elongation of fine grains was by far the most pronounced in AMZIRC; these fine textured grains, combined with precipitation hardening, result in excellent as received strengths at temperatures below 500 °C in AMZIRC. Precipitates in as-received AMZIRC appear coarser than those present in Cu-1Cr-0.1Zr which likely contributes to the higher strength in Cu-1Cr-0.1Zr. Figure 7 shows this fine grain structure in AMZIRC is destroyed at brazing temperatures, and Figure 14 shows the resulting drop in strength.

The microstructures of as received and brazed Cu-1Cr-0.1Zr and Cu-0.9Cr look nearly identical. Recrystallisation appears to have occurred in AMZIRC, Cu-1Cr-0.1Zr, and Cu-0.9Cr during brazing, but, subsequent grain growth and coarsening occurred in AMZIRC only. Chromium appears to have prevented significant grain growth during brazing in the Cu-1Cr-0.1Zr and Cu-0.9Cr alloys. The finer post braze microstructures in Cu-1Cr-0.1Zr and Cu-0.9Cr appear to help little in terms of improved properties. The coarser brazed AMZIRC has about the same strength and creep properties as Cu-1Cr-0.1Zr and Cu-0.9Cr. The differences that stand out among *brazed* Cu-1Cr-0.1Zr, Cu-0.9Cr, and AMZIRC are: AMZIRC has the lowest yield strength (though ultimate strengths are similar); Cu-0.9Cr has significantly poorer creep properties; and as received Cu-0.9Cr had markedly inferior ductility.

### **C. Property Implications on Alloy Selection**

All of the heat treatable alloys (AMZIRC, Cu-1Cr-0.1Zr, and Cu-0.9Cr) have excellent as received properties. The exception observed in this work is that Cu-0.9Cr has relatively poor creep properties in the as received and brazed conditions compared to all the other alloys. Thus if use temperatures are below 500 °C, and no high temperature (>500 °C) processing is required for the alloy, AMZIRC and Cu-1Cr-0.1Zr are advantageous.

The high temperature stability of GlidCop Al-15 and GRCop-84 resulted in superior properties compared to the other alloys in the brazed condition. Ultimate and yield strengths, compressive yield strength, and creep stress at a given strain rate were all about two to three times greater in GlidCop and GRCop-84 compared to the other alloys after the simulated braze heat treatment. Thus if use or processing temperatures in excess of 500 °C are expected, GlidCop Al-15 and GRCop-84 have solid advantages in strength and creep over AMZIRC, Cu-1Cr-0.1Zr, and Cu-0.9Cr.

It may be possible to regain some of the strength lost during the brazing operation in the heat treatable alloys (AMZIRC, Cu-1Cr-0.1Zr, and Cu-0.9Cr). Figure 21 shows that, if the Cu-1Cr-0.1Zr part can be quenched rapidly enough from the brazing temperature (which is also acting as the solution temperature), a significant amount of strength is likely to be regained upon age hardening. If an average cooling rate of 3 K/s can be achieved from the solution temperature throughout the part, and strength and creep gains are proportional to hardness gains, about half of the strength lost resulting from brazing could be mitigated. This would nullify the post braze advantages noted for GlidCop and GRCop-84, but only for use temperatures below 500 °C, or for short term use near 500 °C. As seen in Figure 21, Cu-1Cr-0.1Zr overages as more time is spent at 500 °C. Thus as more time is logged at temperatures near 500 °C and greater, the strength of the heat treatable alloys declines.

#### **D. Future Work**

Planned work will include an analysis of the large precipitates observed in the AMZIRC (Figures 6 and 7) and an attempt to quantify the hardening precipitates (expected to be  $\text{Cu}_5\text{Zr}$ ) before and after brazing. The relative contributions of the three strengthening mechanisms in the heat treatable alloys (1. dislocation (strain), 2. microstructure (grain size), and 3. precipitation hardening) are important because they will determine to what extent strength can be recovered after brazing since only precipitation hardening will be possible after brazing. If a majority of the alloy's strength is due to work and microstructure hardening mechanisms, only slight strength recovery can be expected from post braze precipitation hardening.

#### **V. Summary and Conclusions**

In the as-received condition at <500 °C, AMZIRC, GlidCop Al-15, Cu-1Cr-0.1Zr, and Cu-0.9Cr were all stronger in tension and compression than GRCop-84. However, after a simulated braze heat treatment at 935 °C (1715 °F), the strengths of the precipitation strengthened AMZIRC, Cu-1Cr-0.1Zr and Cu-0.9Cr drop to levels significantly below the strength of GRCop-84 at all temperatures. The strength of dispersion strengthened GlidCop Al-15 was largely unaffected by the heat treatment at 935 °C, thus GlidCop retained strength levels above those of GRCop-84 at all temperatures.

Ductility was lowest in as received Cu-0.9Cr. Ductility was also low for GlidCop Al-15 and in HIPed GRCop-84. The reduction in area was particularly low in GlidCop Al-15 above 500 °C (932 °F). Cu-1Cr-0.1Zr and AMZIRC had much greater reductions in area and elongations than the other alloys.

Creep properties were best for as received Cu-1Cr-0.1Zr and GlidCop Al-15 and worst for Cu-0.9Cr. After the simulated braze at 935 °C GRCop-84 and GlidCop had markedly better creep properties compared to the other alloys. At equivalent stress and strain rates, GRCop-84 showed a 150 °C (302 °F) advantage over AMZIRC in the brazed condition. Alternatively, at

equivalent temperature and strain rates, GRCo-84 was twice as strong as brazed AMZIRC. Our tests indicate GlidCo Al-15 to be more resistant to creep at 500 °C than GRCo-84, with creep rates two orders of magnitude lower than GRCo-84's at equivalent stress.

This work has found that:

- After brazing, GRCo-84 and GlidCo Al-15 are stronger than AMZIRC, Cu-1Cr-0.1Zr, and Cu-0.9Cr;
- After brazing, GRCo-84 and GlidCo Al-15 are superior to AMZIRC, Cu-1Cr-0.1Zr, and Cu-0.9Cr in high temperature creep;
- Due to better ductility and processing characteristics GRCo-84 has advantages over GlidCo Al-15;
- The heat treatment used might be a worst case example for the heat treatable alloys (AMZIRC, Cu-1Cr-0.1Zr, and Cu-0.9Cr). Although strength gained from cold work will be lost at brazing temperatures, it might be possible to recuperate some strength by combining solutionizing, quenching and aging cycles with the brazing operation.

## Tables

Table 1. Composition of Cu alloys in weight percent.

Alloy	Cr	Nb	Zr	Al	O	Ag
GRCo-84	6.65	5.85				
AMZIRC (C15000)			0.15			
GlidCo Al-15 (C15715)				0.15	0.17	
Cu-0.9Cr (C18200)	0.9					
Cu-1Cr-0.1Zr (C18150)	1.0		0.1			
NARLOY-Z			0.5			3.0

Table 2. Simulated braze heat treatment.

Stage	Action
1	Raise temperature from 25 °C to 935 °C
2	Hold at 935 °C for 22.5 ± 2.5 min
3	Lower temperature from 935 °C to 871 °C at 1.7 °C/min
4	Lower temperature from 871 °C to 538 °C at 2.8 °C/min
5	Free cool to room temperature and remove specimen from furnace

Table 3. Ultimate Tensile Stress (UTS) in units of MPa for GRCop-84, AMZIRC, GlidCop Al-15, Cu-1Cr-0.1Zr, and Cu-0.9Cr alloys at various test temperatures; numbers in the table are averages of multiple tests, five tests at each temperature for GRCop-84, most others are the average of two tests.

Temperature °C	As Received GRCop-84	Braze 935 GRCop-84	As Received AMZIRC	Braze 935 AMZIRC	As Received GlidCop	Braze 935 GlidCop	As Received CuCrZr	Braze 935 CuCrZr	As Received CuCr	Braze 935 CuCr
25	368.0	361.0	510.9	233.0	464.5	408.1	564.4	266.3	495.2	245.1
200	257.8	245.4	444.4	180.7	338.3	302.2	487.2	205.9	408.1	186.0
400	203.1	196.2	345.2	153.2						
500			265.3	105.9	184.2	174.5	293.9	89.4	206.5	62.5
600	105.9	100.0	45.3	54.2						
650			33.5	36.1	126.3	124.9	119.5	46.3	104.0	32.0
800	36.2	34.1	15.1	16.9	70.4	69.7	21.2	21.5	25.3	17.4

Table 4. Yield Stress (YS) in units of MPa defined as the stress at 0.2% off-set strain, for GRCop-84, AMZIRC, GlidCop Al-15, Cu-1Cr-0.1Zr, and Cu-0.9Cr alloys at various test temperatures; numbers in the table are averages of multiple tests, five tests at each temperature for GRCop-84, most others are the average of two tests.

Temperature °C	As Received GRCop-84	Braze 935 GRCop-84	As Received AMZIRC	Braze 935 AMZIRC	As Received GlidCop	Braze 935 GlidCop	As Received CuCrZr	Braze 935 CuCrZr	As Received CuCr	Braze 935 CuCr
25	196.2	187.0	501.9	32.8	464.5	408.1	549.9	105.9	441.8	89.7
200	172.3	157.6	438.5	26.9	338.3	302.2	452.2	93.8	396.1	77.6
400	139.5	125.9	342.9	24.5						
500			262.9	25.2	184.2	174.5	283.2	66.4	206.4	42.7
600	87.1	83.0	39.8	22.7						
650			28.8	17.2	126.3	124.9	112.6	35.9	100.5	23.4
800	27.1	28.2	14.0	10.1	70.4	69.7	19.9	19.2	21.7	14.6

Table 5. Elongation, in units of %, defined as the change in gage length divided by the initial gage length times 100%, for GRCoP-84, AMZIRC, GlidCop Al-15, and Cu-1Cr-0.1Zr alloys at various test temperatures; numbers in the table are averages of multiple tests, five tests at each temperature for GRCoP-84, most others are the average of two tests.

Temperature °C	As Received GRCoP-84	Braze 935 GRCoP-84	As Received HIPed GRCoP-84	Braze 935 HIPed GRCoP-84	As Received AMZIRC	Braze 935 AMZIRC	As Received GlidCop Al-15	Braze 935 GlidCop Al-15	As Received CuCrZr	Braze 935 CuCrZr	As Received CuCr	Braze 935 CuCr
25	21.7	25.5	19.2	19.6	19.5	45.6	20.5	25.2	11.2	34.6	18.3	36.7
200	19.5	24.5	24.1	25.4	19.3	44.8	20.9	25.8	17.4	34.1	9.6	34.4
400	17.0	17.3	12.5	12.5	20.1	28.9						
500					21.2	39.8	18.4	18.3	20.3	45.9	1.6	31.4
600	19.8	18.2	9.1	10.2	79.3	47.5						
650					82.4	56.7	9.8	13.2	20.7	41.5	2.8	26.6
800	20.3	18.0	4.9	4.7	64.6	44.7	12.8	16.6	41.8	46.7	9.6	25.2

Table 6. Reduction in area (R/A) in units %, defined as the change in cross-sectional area divided by the initial area times 100%, for GRCoP-84, AMZIRC, GlidCop Al-15, and Cu-1Cr-0.1Zr alloys at various test temperatures; numbers in the table are averages of multiple tests, five tests at each temperature for GRCoP-84, most others are the average of two tests.

Temperature °C	As Received GRCoP-84	Braze 935 GRCoP-84	As Received AMZIRC	Braze 935 AMZIRC	As Received GlidCop Al-15	Braze 935 GlidCop Al-15	As Received CuCrZr	Braze 935 CuCrZr	As Received CuCr	Braze 935 CuCr
25	39.7	40.6	57.2	76.0	74.1	80.9	62.6	79.2	60.1	70.5
200	59.0	59.6	54.6	72.1	38.3	65.8	49.9	76.8	21.6	65.7
400	28.0	33.5	58.6	46.4						
500			62.9	49.8	21.2	24.5	38.1	78.2	7.0	29.6
600	28.4	30.6	49.2	38.8						
650			52.8	41.9	11.9	15.0	15.5	47.9	6.4	24.4
800	28.7	28.8	49.1	38.6	11.8	11.8	37.8	46.0	11.5	23.5

Table 7. Compressive Yield Strength, in units MPa, defined as the compressive stress at 0.2% off-set strain, for GRCop-84, AMZIRC, GlidCop Al-15, Cu-1Cr-0.1Zr, and Cu-0.9Cr alloys at various test temperatures; numbers in the table are averages of multiple tests, two or three tests at each temperature for GRCop-84, all of the values for the other alloys are the average of two tests.

Test Temperature (°C)	GRCop-84 As Received	AMZIRC As Received	AMZIRC Braze 935	GlidCop As Received	GlidCop Braze 935	Cu-Cr-Zr As Received	Cu-Cr-Zr Braze 935	Cu-Cr As Received	Cu-Cr Braze 935
23.0	311.8	464.0	111.0	432.9	348.3	501.4	94.0	450.0	93.2
350.0	166.6	365.7	64.1	241.6	204.8	379.9	67.0	307.4	55.5
500.0	118.3	273.6	38.7	160.0	152.3	259.2	47.5	221.1	33.0
650.0	66.7	27.7	16.2	103.0	102.3	96.2	30.1	83.4	19.9
800.0	24.1	9.6	9.7	52.2	52.0	18.1	15.9	15.6	11.4

Table 8. Step Loaded, Creep Strain Rates at various temperatures, in units of strain/second, with 5 hours at each stress listed, for up to 20 steps, or failure. Creep, or strain rate, was defined as the slope of the time-strain data at the inflection point between primary and tertiary creep.

GRCop-84 as received, 500 °C		GRCop-84 as received, 650 °C		GRCop-84 as received, 800 °C			
Stress, MPa	Strain Rate, /sec	Stress, MPa	Strain Rate, /sec	Stress, MPa	Strain Rate, /sec		
15.96	1.58E-08	2.49	2.49E-09	4.49	2.14E-09		
21.98	1.65E-08	4.98	5.51E-09	4.99	2.55E-09		
27.98	1.23E-08	7.47	7.08E-09	5.45	1.35E-08		
30.98	1.31E-08	9.96	8.22E-09	5.49	1.41E-09		
33.01	3.64E-09	12.45	1.73E-08	6.20	2.68E-08		
33.97	1.50E-08	14.98	8.63E-09	6.29	4.79E-09		
36.03	9.84E-10	17.43	2.01E-08	6.95	3.87E-08		
36.97	9.34E-09	17.49	8.42E-09	6.98	7.11E-09		
39.43	1.71E-09	19.93	3.08E-08	7.09	7.54E-09		
39.96	1.23E-08	19.99	1.46E-08	7.71	4.19E-08		
39.97	6.60E-09	22.42	4.07E-08	7.99	7.84E-09		
42.96	9.66E-09	22.48	1.92E-08	8.48	3.93E-09		
42.98	1.41E-08	24.91	4.19E-08	8.48	2.44E-08		
43.03	1.88E-09	24.98	2.17E-08	8.98	2.30E-09		
45.96	1.10E-08	27.40	2.32E-08	9.09	9.53E-09		
45.96	2.16E-08	27.48	3.60E-08	9.21	1.88E-08		
47.04	5.57E-09	29.89	3.02E-08	9.48	8.05E-09		
48.38	6.70E-09	29.98	4.34E-08	9.96	3.99E-08		
51.96	2.58E-08	32.40	4.48E-08	10.19	1.45E-08		
51.96	1.21E-08	32.48	6.24E-08	10.47	7.78E-09		
54.96	1.98E-08	34.87	8.56E-08	10.71	3.84E-08		
54.96	1.52E-08	34.98	8.12E-08	10.97	1.12E-08		
56.04	6.35E-09	37.36	1.10E-07	11.46	3.94E-08		
57.95	1.99E-08	37.47	1.11E-07	11.47	7.99E-09		
57.96	3.52E-08	39.84	2.19E-07	11.49	1.80E-08		
60.95	2.90E-08	39.95	3.84E-07	11.97	6.73E-09		
60.96	2.84E-08	39.99	1.83E-07	12.22	5.50E-08		
61.25	5.97E-09	42.34	3.59E-07	12.47	1.46E-08		
63.95	1.86E-08	42.47	3.06E-07	12.97	4.75E-08		
63.95	2.98E-08	42.47	5.50E-07	12.97	2.88E-08		
66.95	2.26E-08	44.83	6.37E-07	12.99	2.13E-08		
66.95	2.94E-08	44.96	9.59E-07	13.01	1.09E-07		
66.95	1.50E-08	44.97	5.15E-07	13.72	7.59E-08		
69.95	3.95E-08	47.34	1.24E-06	13.74	8.79E-08		
72.94	2.32E-08	47.46	2.07E-06	13.89	4.15E-08		



Table 8. continued from previous page, step loaded creep.

72.94	3.52E-08	47.46	1.00E-06	14.47	6.47E-08		
73.06	2.64E-08	49.81	2.65E-06	14.53	4.90E-08		
75.66	3.76E-08	49.84	4.72E-06	14.89	6.62E-08		
75.94	4.49E-08	49.95	2.19E-06	15.22	7.71E-08		
75.94	2.58E-08	52.51	4.94E-06	15.28	6.70E-08		
78.36	3.74E-08			15.98	1.12E-07		
78.91	3.66E-08			15.98	1.14E-07		
78.94	6.76E-08			16.04	9.20E-08		
81.17	3.90E-08			16.72	1.28E-07		
81.93	6.07E-08			16.79	9.39E-08		
81.94	8.98E-08			17.08	1.96E-07		
84.07	8.04E-08			17.47	1.70E-07		
84.94	1.14E-07			17.55	1.37E-07		
84.94	1.38E-07			18.22	2.27E-07		
87.07	1.08E-07			18.27	3.68E-07		
87.93	7.46E-08			18.31	1.57E-07		
87.93	1.41E-07			18.98	3.30E-07		
90.16	1.47E-07			19.04	2.80E-07		
90.92	2.70E-07			19.59	7.83E-07		
90.93	1.73E-07			19.73	4.76E-07		
93.34	2.02E-07			19.82	3.12E-07		
93.92	1.91E-07			20.57	3.65E-07		
93.93	2.31E-07			20.97	6.86E-07		
96.66	2.78E-07			21.33	4.55E-07		
96.92	2.45E-07			21.57	1.06E-06		
96.93	2.82E-07			22.08	5.95E-07		
99.91	5.10E-07			22.27	1.70E-06		
100.18	3.87E-07			22.84	8.20E-07		
102.93	6.25E-07			22.87	2.57E-06		
103.68	5.39E-07			23.57	3.93E-06		
105.93	1.20E-06			23.59	1.14E-06		
111.89	1.68E-06			24.27	5.88E-06		
114.90	1.76E-06			24.34	1.73E-06		
117.90	2.33E-06			24.97	9.14E-06		
120.89	3.04E-06			25.10	2.50E-06		
123.90	3.56E-06			25.85	3.76E-06		
126.89	4.54E-06			26.61	5.92E-06		
				27.36	1.06E-05		

Table 8. continued from previous page, step loaded creep strain rates.

AMZIRC as received, 500 °C		AMZIRC Braze 935, 500 °C		AMZIRC as received, 650 °C		AMZIRC Braze 935, 650 °C	
Stress, MPa	Strain Rate, /sec	Stress, MPa	Strain Rate, /sec	Stress, MPa	Strain Rate, /sec	Stress, MPa	Strain Rate, /sec
50	4.40E-08	34	1.40E-07	15.3	7.80E-06	8.35	1.80E-08
50	4.00E-08	36	2.70E-07	16	7.50E-06	9.15	5.90E-08
60	3.65E-08	38	3.27E-07			9.95	1.23E-07
62	4.27E-08	40	4.03E-07			10.75	1.85E-07
70	1.18E-07	42	4.63E-07			11.55	2.85E-07
74	7.26E-08	44	5.76E-07			12.34	3.15E-07
80	4.60E-07	46	6.80E-07			13.14	3.87E-07
86	1.90E-07	48	7.70E-07			13.94	4.44E-07
98	1.20E-06	50	9.24E-07			14.73	5.20E-07
		52	1.43E-06			15.53	5.54E-07
		54	1.57E-06			16.34	6.64E-07
		56	2.43E-06			18	9.15E-07
		58	4.02E-06			19	1.04E-06
		60	8.82E-06			20	1.38E-06
						20.8	1.70E-06
						21.6	2.60E-06
						22.5	4.70E-06
GlidCop as received, 500 °C		GlidCop Braze 935 500 °C		GlidCop as received, 650 °C		GlidCop Braze 935 650 °C	
Stress, MPa	Strain Rate, /sec	Stress, MPa	Strain Rate, /sec	Stress, MPa	Strain Rate, /sec	Stress, MPa	Strain Rate, /sec
111.2	2.51E-08	104.7	2.92E-08	69.7	4.31E-08	70	3.57E-08
115.4	2.50E-08	108.7	2.92E-08	71.7	3.61E-08	72	2.92E-08
119.5	3.30E-08	112.6	4.60E-08	73.7	3.75E-08	74	4.38E-08
123.6	3.70E-08	116.7	3.22E-08	75.7	3.75E-08	76	3.72E-08
127.8	4.38E-08	120.6	3.46E-08	77.7	3.75E-08	78	4.96E-08
131.9	4.44E-08	124.6	4.22E-08	79.7	2.57E-08	80	4.18E-08
136.1	6.25E-08	128.6	5.85E-08	81.7	3.06E-08	82	4.83E-08
140.2	8.95E-08	132.6	6.36E-08	83.7	3.06E-08	84	7.25E-08
144.3	2.10E-07	136.7	8.70E-08	85.7	3.04E-08	86	6.60E-08
148.5	4.00E-07	140.6	1.44E-07	87.7	4.58E-08	88	1.03E-07
152.6	1.35E-06	144.7	3.14E-07	89.7	5.28E-08	90	1.50E-07
				91.7	4.44E-08	92	2.83E-07
				93.7	9.65E-08		
				95.7	1.39E-07		
				97.7	2.04E-07		
				99.7	3.04E-07		

Table 8. continued from previous page, step loaded creep strain rates.

CuCrZr as received, 500 °C		CuCrZr Brazed, 500 °C		CuCrZr as received, 650 °C		CuCrZr Brazed, 650 °C	
Stress, MPa	Strain Rate, /sec	Stress, MPa	Strain Rate, /sec	Stress, MPa	Strain Rate, /sec	Stress, MPa	Strain Rate, /sec
87	2.28E-08	29.5	1.00E-08	20	3.61E-07	9.6	8.05E-09
94	1.59E-08	32	1.00E-08	24	8.19E-07	11.2	1.03E-08
101	2.41E-08	34.5	1.94E-08	28	1.97E-06	14.4	3.65E-08
108	3.98E-08	37	6.80E-08			16	8.15E-08
115	4.65E-08	39.5	7.39E-08			17.6	1.02E-07
122	5.63E-08	42	1.08E-07			19.2	1.92E-07
129	1.12E-07	44.5	1.99E-07			20.8	2.56E-07
136	1.34E-07	47	1.87E-07			22.4	2.65E-07
143	1.74E-07	49.5	2.44E-07			24	6.13E-07
150	2.26E-07	52	3.61E-07			25.6	1.04E-06
155	1.75E-07	54.5	4.28E-07			27.2	1.77E-06
164	4.76E-07	57	5.94E-07			28.8	6.42E-06
171	1.55E-06	59.5	7.44E-07				
		62	9.60E-07				
		64.5	1.14E-06				
		67	1.78E-06				
		69.5	2.93E-06				
		72	5.45E-06				
		74.5	1.27E-05				
CuCr as received, 500 °C		CuCr Brazed, 500 °C		CuCr as received, 650 °C		CuCr Brazed, 650 °C	
Stress, MPa	Strain Rate, /sec	Stress, MPa	Strain Rate, /sec	Stress, MPa	Strain Rate, /sec	Stress, MPa	Strain Rate, /sec
40	5.56E-08	16	9.81E-08	24	6.66E-06	7	3.35E-07
45	7.26E-08	18	1.21E-07			8	4.36E-07
50	1.33E-07	20	1.78E-07			9	5.91E-07
55	2.01E-07	22	2.44E-07			10	8.87E-07
60	4.39E-07	24	3.78E-07			11	1.18E-06
65	1.29E-06	26	5.67E-07			12	1.65E-06
		28	1.00E-06			13	2.32E-06
		30	2.53E-06			14	3.33E-06
						15	5.39E-06

Table 9. Power function constants for step loaded, secondary steady state creep; creep rate power functions of the form  $\dot{\epsilon} = A\sigma^n$  where  $A$  and  $n$  are given in the table,  $\dot{\epsilon}$  is creep rate in units of  $\text{sec}^{-1}$ , and  $\sigma$  is step loaded creep stress in units of MPa.

	$A$	$n$
GRCop-84 as received, 500 °C	4.77E-26	9.49
GRCop-84 as received, 650 °C	7.17E-24	10.32
GRCop-84 as received, 800 °C	2.63E-18	8.67
AMZIRC as received, 500 °C	4.15E-20	6.70
AMZIRC Brazed, 500 °C	4.18E-13	3.73
AMZIRC as received, 650 °C	*	*
AMZIRC Brazed, 650 °C	2.99E-11	3.65
GlidCop as received, 500 °C	7.71E-57	22.93
GlidCop Brazed, 500 °C	3.72E-34	12.40
GlidCop as received, 650 °C	4.58E-39	15.90
GlidCop Brazed, 650 °C	8.48E-38	15.50
Cu-1Cr-0.1Zr as received, 500 °C	1.47E-19	5.59
Cu-1Cr-0.1Zr Brazed 500 °C	5.94E-17	5.71
Cu-1Cr-0.1Zr as received 650 °C	1.01E-13	5.03
Cu-1Cr-0.1Zr Brazed 650 °C	1.50E-14	5.52
Cu-0.9Cr as received 500 °C	7.31E-18	6.04
Cu-0.9Cr Brazed, 500 °C	4.00E-14	5.08
Cu-0.9Cr as received 650 °C	*	*
Cu-0.9Cr Brazed 650 °C	1.27E-10	3.83

\* Insufficient data to obtain constants

Table 10. Constant load, steady state creep rate and creep life to failure; stress is initial stress based on initial cross sectional area. Creep, or strain rate, was defined as the slope of the time-strain data at the inflection point between primary and tertiary creep.

GRCop-84 as received, 500 °C		GRCop-84 Brazed, 500 °C		GRCop-84 as received, 650 °C		GRCop-84 Brazed, 650 °C		GRCop-84 as received, 800 °C		GRCop-84 Brazed, 800 °C	
Stress, MPa	Life, hours	Stress, MPa	Life, hours	Stress, MPa	Life, hours	Stress, MPa	Life, hours	Stress, MPa	Life, hours	Stress, MPa	Life, hours
72.9	660.12	99	52.24	37.4	649.63	37.4	25.65	17.4	16.88	15.4	20.14
72.9	446.44	99	193.78	37.4	135.08	37.4	16.92	17.4	20.32	15.4	35.82
72.9	528.67	99	3.9	37.4	108.41	37.4	9.83	17.4	15.3	15.4	27.76
72.9	272.18	99	9.15	37.4	188.45	37.4	7.85	17.4	19.4	15.4	39.61
72.9	375.15	99	17.52	37.4	111.57	37.4	64.04	17.4	29.53	15.4	18.19
72.9	1269.22	104.2	45	37.4	530.43	44.3	2.29	19.2	89.57	17.4	2.48
84	556.03	109	5.75	44.3	114.93	44.3	11.4	19.2	62.28	17.4	4.88
84	357.28	109	67.1	44.3	23.94	44.3	2.25	19.2	48.95	17.4	16.32
84	119.51	109	34.77	44.3	32.43	44.3	10.69	19.2	49.68	17.4	7.87
84	188.23	109	19.49	44.3	45.42	44.3	9.97	19.2	38.52	17.4	12.83
84	124.09	119	0.73	44.3	75.2	45.1	3.79	19.2	38.7	19.3	9.16
84	148.59	119	0.93	44.3	40.28	51.2	1.06	19.3	10.8	19.3	10
92.8	671.65	119	4.14	44.3	14.77	51.2	1.21	19.3	8.9	19.3	5.18
92.8	32.89	119	1.1	44.3	11.33	51.2	1.29	19.3	9	19.3	7.36
92.8	70.39	125.1	0.16	44.3	11.62	51.2	8.34	19.3	7.1	19.3	2.07
92.8	43.45			44.3	30.15	53.8	0.31	19.3	10.8		
92.8	578.03			44.3	8.9	63.2	0.31	23.2	4		
92.8	39.32			49.8	76.99			23.2	1.7		
109	33.13			49.8	19.33			23.2	2.3		
109	4.89			49.8	21.19			23.2	7		
109	29.15			49.8	12.5			23.2	4.6		
109	4.58			49.8	14.13			23.3	39.97		
109	3.68			49.8	39.32			23.3	8.55		
119	8.1			51.2	4.4			23.3	18.52		

Table 10. continued from previous page, constant load creep.

119	25.3			51.2	2.3				23.3	8.7		
119	3.6			51.2	2.8				23.3	9.4		
119	7.7			51.2	6.1				23.3	20.13		
119	2.9			51.2	2.8				26.8	12.97		
133	27			57.2	5				26.8	4.96		
133	8.8			57.2	4.8				26.8	5.41		
133	14.6			57.2	4.8				26.8	3.1		
133	5.1			57.2	1.4				26.8	6.97		
133	2			57.2	4.9				26.8	5.3		
147	0.3			63.2	5.4				27.3	2.9		
147	1.5			63.2	1				27.3	1.9		
147	3.8			63.2	3.1				27.3	1		
147	1			63.2	6.9				27.3	0.6		
147	1.8			63.2	2.5				27.3	1.2		
AMZIRC as received, 500 °C												
Stress, MPa	Life, hours	Strain Rate, /sec	Stress, MPa	Life, hours	Strain Rate, /sec	Stress, MPa	Life, hours	Strain Rate, /sec	Life, hours	Stress, MPa	Life, hours	Strain Rate, /sec
87	38.6	3.77E-08	AMZIRC Brazed, 500 °C	60	1.51E-06	11	69.1	1.29E-06	25	19.3	1.86E-06	
120	22.08	6.74E-08	60	22.8	2.30E-06	15	20	3.70E-06	27	13.9	2.82E-06	
140	15.7	9.20E-08	65	43.8	7.04E-07	16.5	12.2	6.15E-06	30	6	7.58E-06	
170	16.3	1.08E-07	65	26	2.09E-06	18	9.1	1.02E-05				
210	5.3	3.64E-07	70	10.24	6.97E-06	20	8.5	8.80E-06				
			75	6.2	1.40E-05							

continued

Table 10. continued from previous page, constant load creep.

GlidCop as received, 500 °C	Life, hours	Strain Rate, /sec	GlidCop, Brazed, 500 °C	Life, hours	Strain Rate, /sec	GlidCop, as received, 650 °C	Life, hours	Strain Rate, /sec	GlidCop, Brazed, 650 °C	Life, hours	Strain Rate, /sec
Stress, MPa	46.34	5.00E-08	Stress, MPa	168	8.61E-09	Stress, MPa	57.8	1.67E-08	Stress, MPa	155	6.08E-09
149.6	28.3	6.57E-08	144	24.7	8.33E-08	93	16.6	7.97E-08	84	19.38	1.03E-07
155	6.5	6.00E-07	147.5	9.2	3.53E-07	100	2.36	1.44E-06	90	13	1.90E-07
160			150			110			95	6.47	3.96E-07
									99		
CuCrZr, as received, 500 °C			CuCrZr, Brazed, 500 °C			CuCrZr, as received, 650 °C			CuCrZr, Brazed, 650 °C		
Stress, MPa	Life, hours	Strain Rate, /sec	Stress, MPa	Life, hours	Strain Rate, /sec	Stress, MPa	Life, hours	Strain Rate, /sec	Stress, MPa	Life, hours	Strain Rate, /sec
140	150	2.51E-08	67	21.7	2.60E-06	25	27.9	3.68E-07	25	54.8	5.65E-07
156	33.2	7.90E-08	73	7.41	8.51E-06	30	11	6.92E-07	30	13	3.41E-06
170	19.5	1.55E-07	79	8.7	7.00E-06	34	8.1	6.88E-07	32	16.8	2.36E-06
178	14.1	2.22E-07	84	4.8	8.22E-06				34	7.53	5.88E-06
185	14.5	1.94E-07									
195	22.3	9.00E-08									
210	8.2	3.95E-07									

continued

Table 10. continued from previous page, constant load creep.

CuCr, as received, 500 °C		CuCr, Brazed, 500 °C		CuCr, as received, 650 °C		CuCr, Brazed, 650 °C	
Stress, MPa	Life, hours	Strain Rate, /sec	Life, hours	Strain Rate, /sec	Life, hours	Strain Rate, /sec	Life, hours
57	30.2	1.23E-07	51.2	9.50E-07	10	8.52E-07	80.7
65	18	2.02E-07	28.4	1.65E-06	15	2.13E-06*	22.9
73	12	2.59E-07	18.6	3.00E-06	19	5.20E-07*	7.35
			13.8	2.97E-06	22	5.73E-07*	

\* CuCr strain rates marked with an \* were included for completeness – there was no significant secondary creep in these runs – the strain rates listed are the slopes of the strain/time plot at the inflection between primary and tertiary creep.



Table 11. Power function constants for constant load, secondary, steady state tensile creep at elevated temperatures; creep rate power functions of the form  $\dot{\epsilon} = A\sigma^n$  where  $A$  and  $n$  are given in the table,  $\dot{\epsilon}$  is creep rate in units of  $\text{sec}^{-1}$ , and  $\sigma$  is constant load creep stress in units of MPa.

	$A$	$n$
GRCop-84, 500 °C	1.042E-22	7.67
GRCop-84 650 °C	3.400E-21	8.52
GRCop84 800 °C	1.078E-16	7.3
Amzirc as received, 500 °C	8.919E-13	2.35237
Amzirc Brazed, 500 °C	1.633E-23	9.48610
Amzirc as received, 650 °C	2.638E-10	3.55738
Amzirc Brazed, 650 °C	2.141E-17	7.80399
GlidCop as received, 500 °C	2.392E-87	36.40497
GlidCop Brazed, 500 °C	1.195E-205	91.21151
GlidCop as received, 650 °C	3.312E-61	26.74301
GlidCop Brazed, 650 °C	2.762E-56	24.69575
CuCrZr as received, 500 °C	6.857E-20	5.46637
CuCrZr Brazed 500 °C	2.489E-14	4.46268
CuCrZr as received 650 °C	4.040E-10	2.13871
CuCrZr Brazed 650 °C	8.059E-17	7.07106
CuCr as received 500 °C	6.353E-13	3.01887
CuCr Brazed, 500 °C	7.363E-13	4.17238
CuCr as received 650 °C	*	*
CuCr Brazed 650 °C	6.047E-11	4.05855

\* Did not follow power law creep.

Table 12. Thermal Expansion of AMZIRC, GlidCop Al-15, Cu-1Cr-0.1Zr, and Cu-0.9Cr alloys where the thermal expansion,  $\alpha$ , in units of in/in, is expressed as a quadratic function of temperature,  $T$ , in units of °C, such that  $\alpha(T) = A(T)^2 + B(T) + C$ . Based on the variations of  $\alpha$  expressed among different specimens,  $\alpha$  values are estimated to be accurate to within  $\pm 1\%$ .

Alloy	A	B	C
AMZIRC	4.132E-09	1.610E-05	-1.701E-04
GlidCop Al-15	3.989E-09	1.619E-05	-1.000E-04
Cu-1Cr-0.1Zr	4.947E-09	1.559E-05	-8.019E-05
Cu-0.9Cr	4.317E-09	1.599E-05	-1.016E-04

Table 13. Summary and comparison of alloy properties.

Property	Comparison
Thermal conductivity	The conductivity of oxygen free copper is about 400 W/mK, all alloys of copper are below this value. The conductivity of AMZIRC is best at about 370 W/mK, the conductivity of GlidCop Al-15 and NARloy-Z is approximately 320 W/mK, and that of GRCop-84 is about 300 W/mK [3].
Thermal expansion	The thermal expansion of GRCop-84 is the lowest at 0.008 in/in at 480 °C; the expansion of GlidCop, AMZIRC, Cu-1Cr-0.1Zr, and Cu-0.9Cr at this temperature are all about the same at 0.0087 in/in.
Strength	Since GlidCop and GRCop-84 are not significantly influenced by high temperature brazing, these two alloys are clearly stronger than the heat treatable alloys (AMZIRC, Cu-1Cr-0.1Zr, Cu-0.9Cr) after brazing. In the absence of any brazing heat treatment – Cu-1Cr-0.1Zr is strongest, even at test temperatures up to 650 °C. However, the strength of Cu-1Cr-0.1Zr is expected to degrade with time at use temperatures in excess of 500 °C due to over aging.
Compressive strength	Compressive strength in these alloys closely follow what was found for tensile strength. GlidCop Al-15 and GRCop-84 were the strongest after brazing.
Ductility	GRCop-84, AMZIRC, and Cu-1Cr-0.1Zr all had good ductility. GRCop-84's elongation was the most consistent, remaining between about 16% and 25% across the entire temperature range tested (20 to 800 °C). GlidCop Al-15 and Cu-0.9Cr had the worst ductility at temperatures greater than 500 °C; the ductility of Cu-0.9Cr was particularly bad (~2% elongation) at 500 and 650 °C.
Creep	Based on step loaded creep results, GlidCop Al-15 had the best creep properties of all the alloys regardless of brazing condition. The creep properties of as received Cu-1Cr-0.1Zr were as good as GlidCop's, however, the creep rates of Cu-1Cr-0.1Zr, AMZIRC, and Cu-0.9Cr dropped dramatically after the brazing heat treatment. Thus after brazing, GRCop-84 and GlidCop Al-15 had better creep properties than the other alloys. In the brazed condition, at a strain rate of $10^{-6} \text{ sec}^{-1}$ the step loaded creep stress for GlidCop Al-15 was about 160 MPa; at these same conditions the creep stress was about 110 MPa for GRCop-84, and about 60 MPa for the other three alloys.
Effects of Brazing	GRCop-84 and GlidCop Al-15 were not significantly affected by the simulated braze. AMZIRC, Cu-1Cr-0.1Zr, and Cu-0.9Cr lost their strength due to the braze, with strengths dropping by about 80% or more.

## Figures

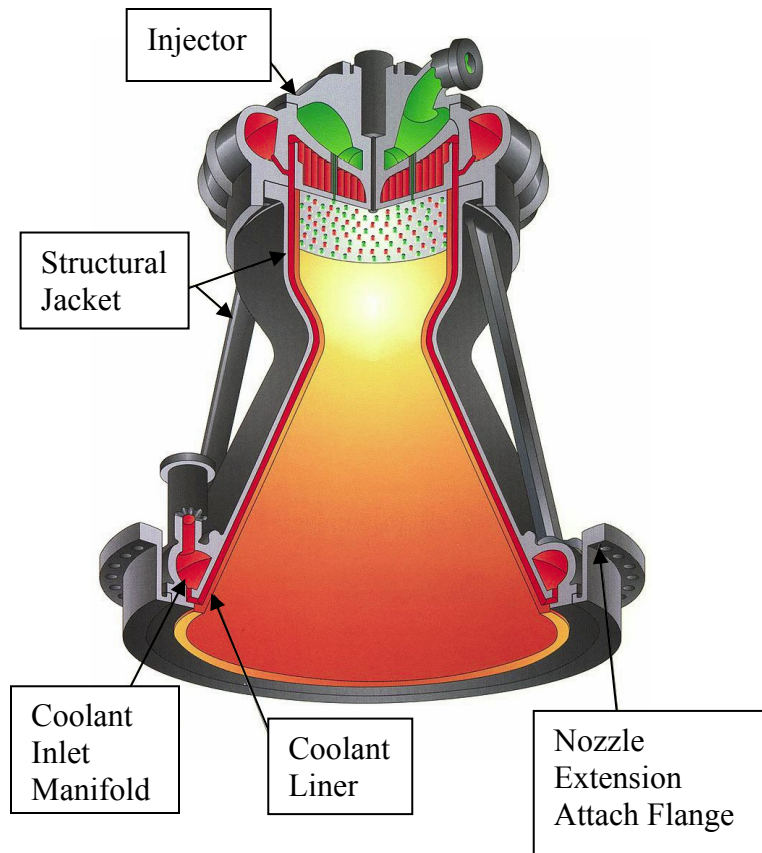


Figure 1. Schematic of regeneratively cooled combustion chamber. (Image used with permission from Pratt & Whitney Rocketdyne, Inc.)

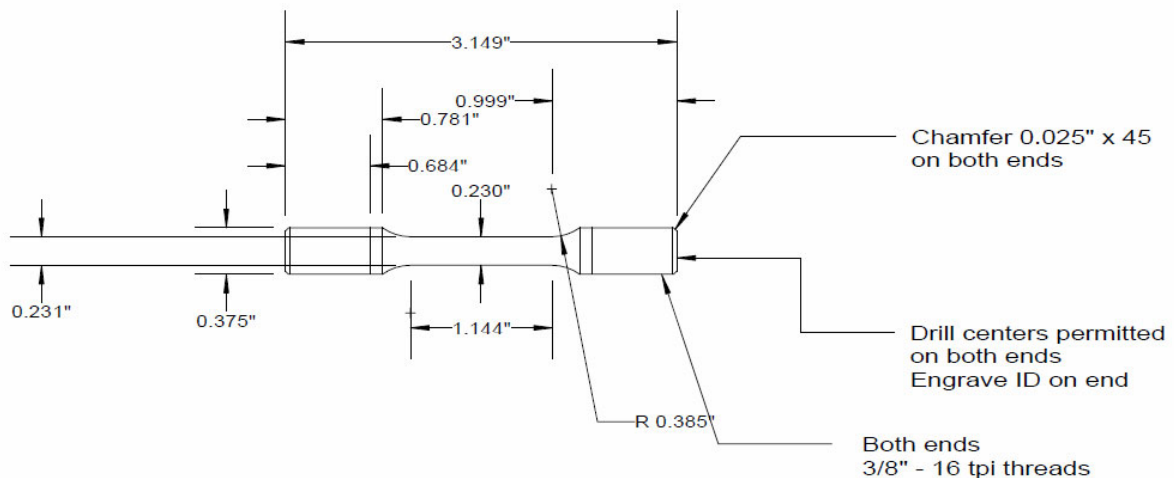


Figure 2. Specimen designed used for AMZIRC tensile and creep specimens.



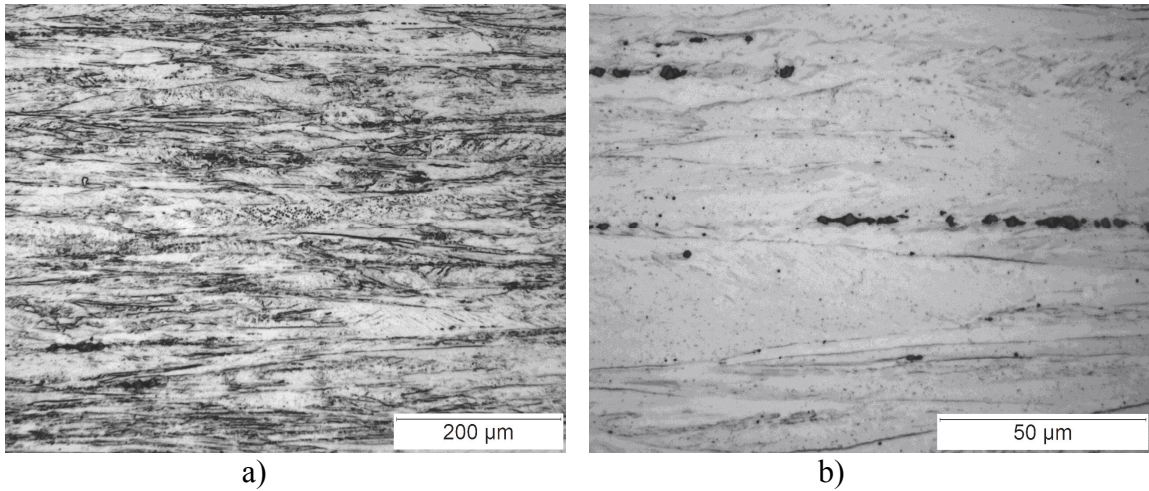


Figure 6. AMZIRC longitudinal microstructures in the as received condition; longitudinal/drawing direction is horizontal; dark spots are likely  $\text{Cu}_5\text{Zr}$ .

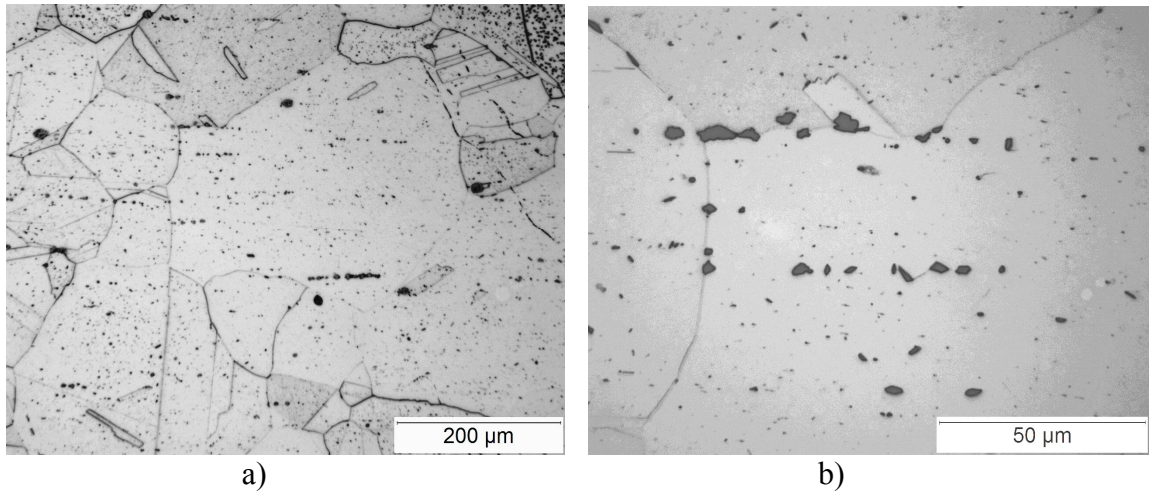


Figure 7. AMZIRC longitudinal microstructures after the simulated brazing heat treatment at  $935\text{ }^\circ\text{C}$ ; longitudinal/drawing direction is horizontal.

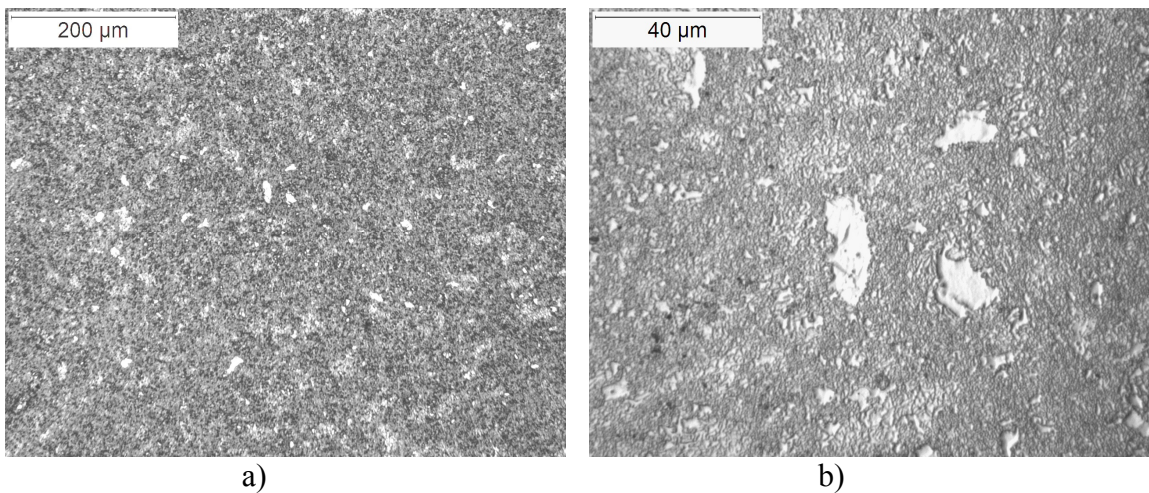


Figure 8. GlidCop Al-15 longitudinal micrograph of the as received condition; longitudinal/drawing direction is horizontal.

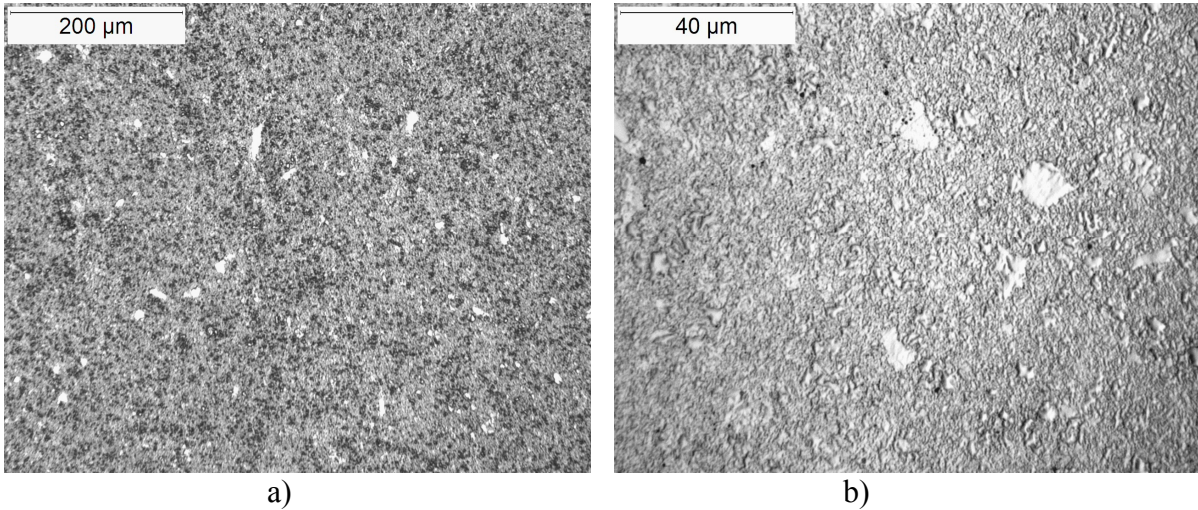


Figure 9. GlidCop Al-15 longitudinal microstructures after the simulated brazing heat treatment at 935 °C; longitudinal/drawing direction is horizontal.

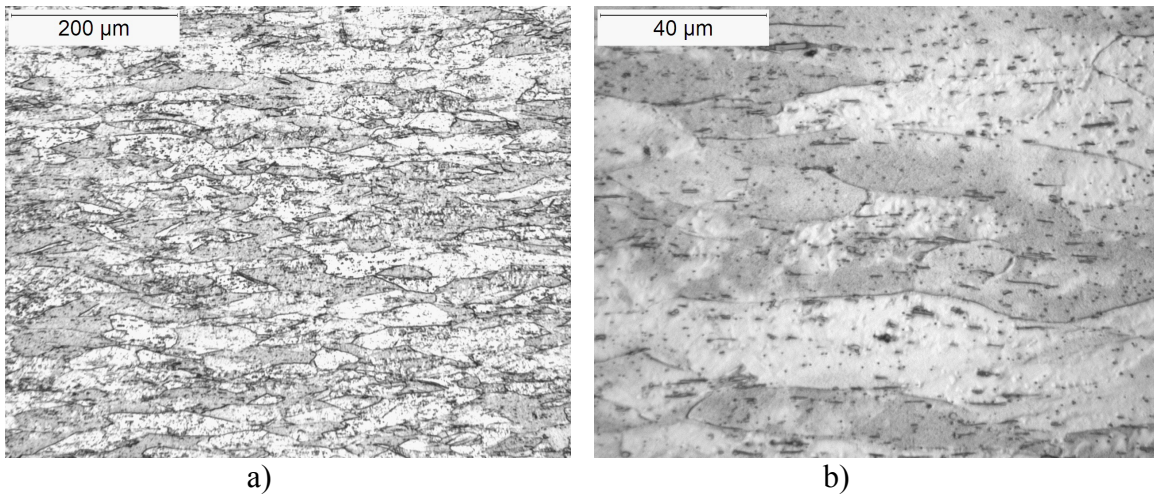


Figure 10. Cu-1Cr-0.1Zr micrograph of the as received condition.

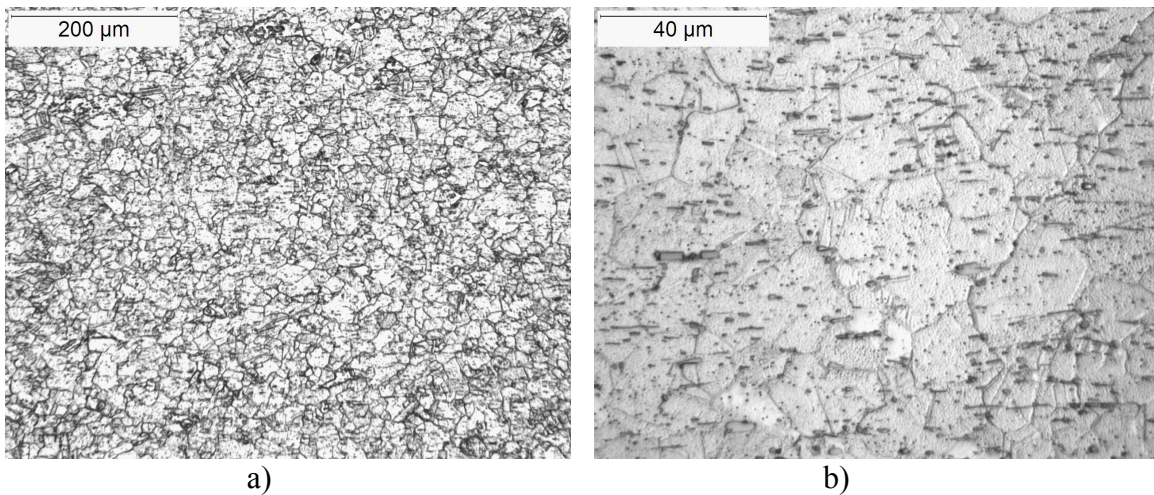
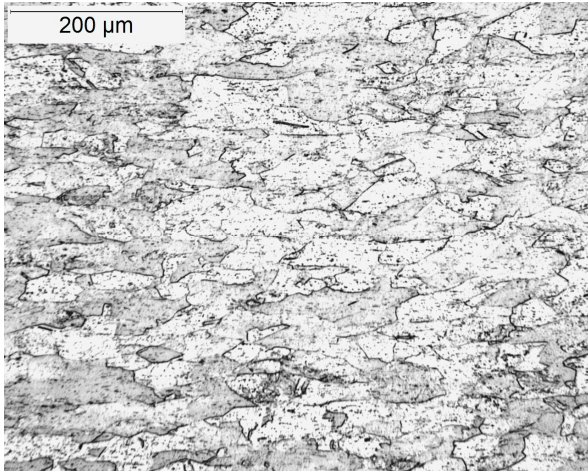
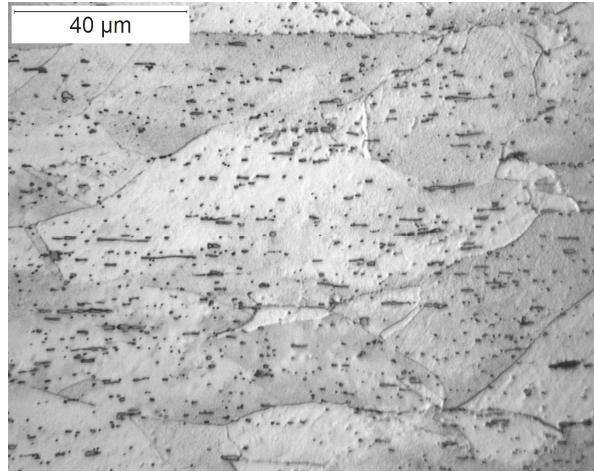


Figure 11. Cu-1Cr-0.1Zr longitudinal microstructures after the simulated brazing heat treatment at 935 °C; longitudinal/drawing direction is horizontal.

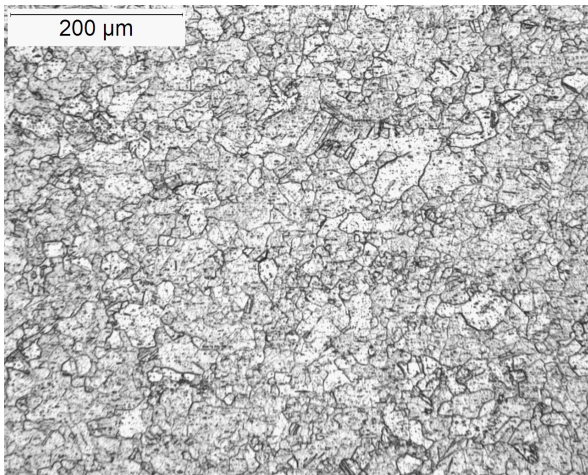


a)

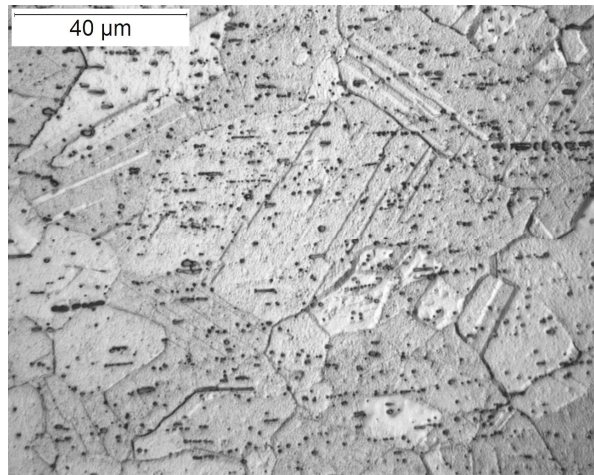


b)

Figure 12. Cu-0.9Cr micrograph of the as received condition.



a)



b)

Figure 13. Cu-0.9Cr micrograph of the brazed condition.

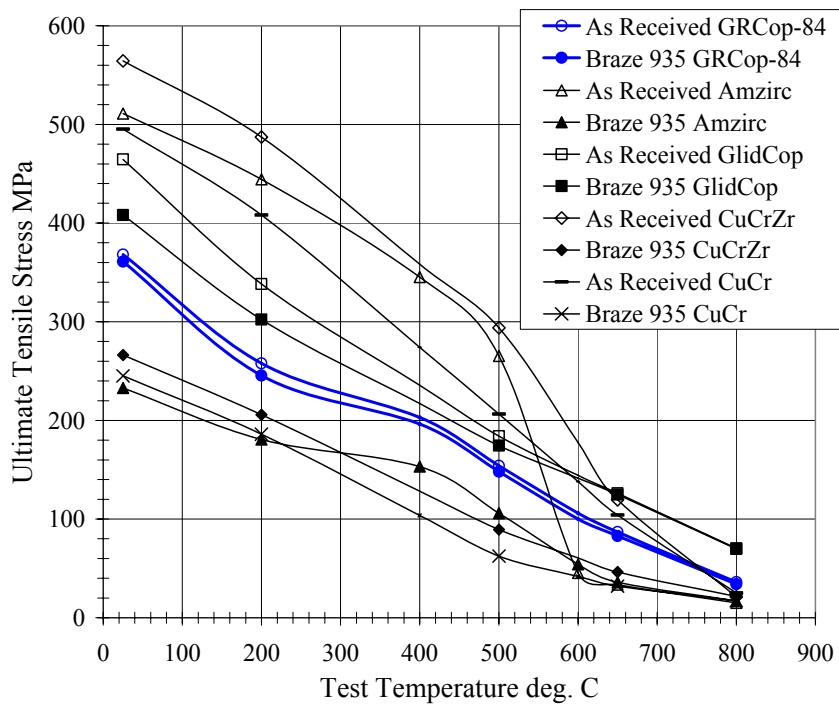


Figure 14. Ultimate tensile stress for as-received and brazed GRCop-84, AMZIRC, GlidCop Al-15, Cu-1Cr-0.1Zr, and Cu-0.9Cr alloys. GRCop-84 values are the average of HIPed and extruded material, data points represent averages of multiple tests, five tests at each temperature for GRCop-84, most others are the average of two tests.

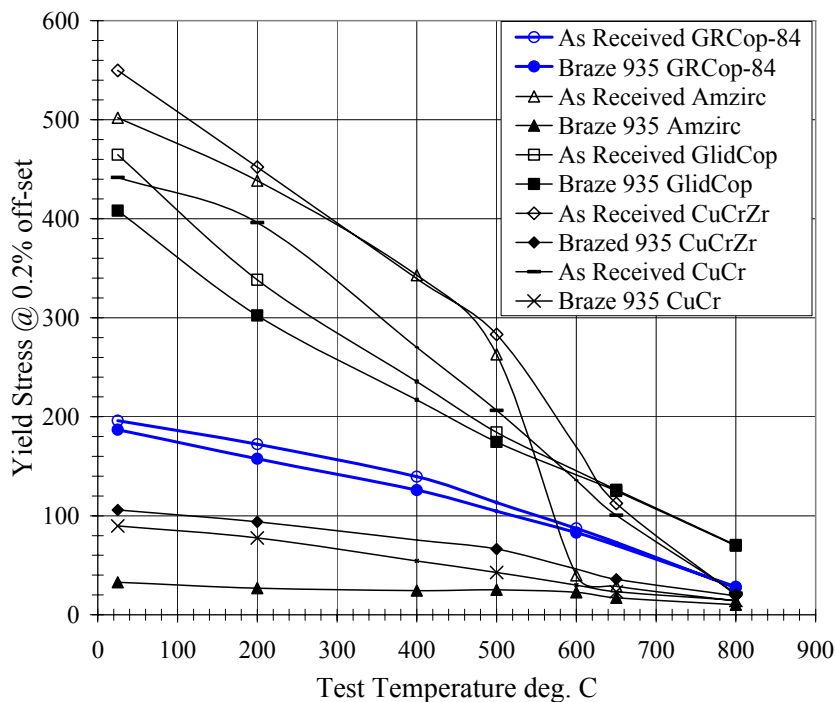


Figure 15. Yield Strength, in units of MPa, at 0.2% off-set strain for as-received and brazed GRCop-84, AMZIRC, GlidCop Al-15, Cu-1Cr-0.1Zr, and Cu-0.9Cr alloys. GRCop-84 values are the average of HIPed and extruded material, data points represent averages of multiple tests, five tests at each temperature for GRCop-84, most others are the average of two tests.



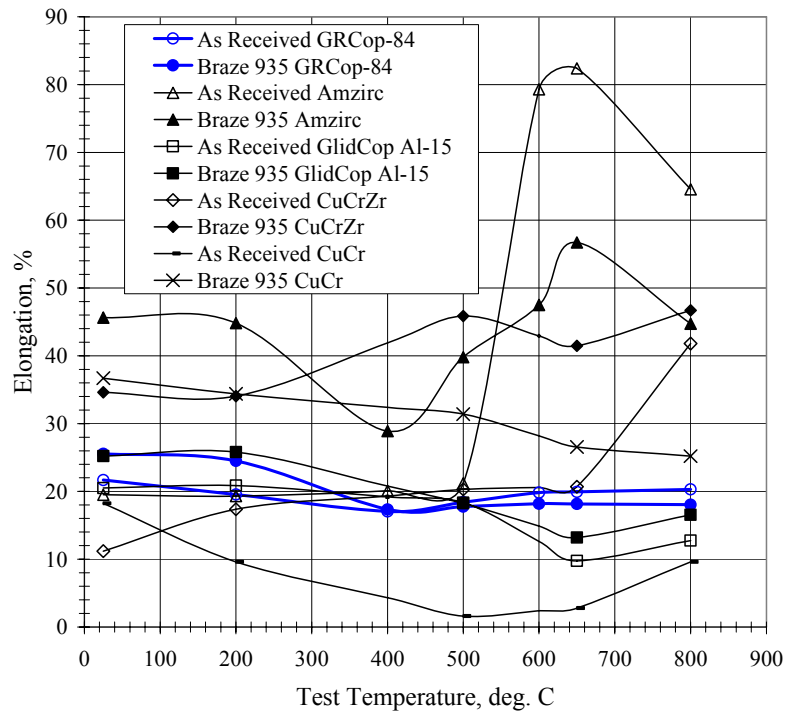


Figure 16. Elongation in tensile of as-received and braze heat treated GRCop-84, AMZIRC, GlidCop Al-15, Cu-1Cr-0.1Zr, and Cu-0.9Cr alloys. Data points represent averages of multiple tests, five tests at each temperature for GRCop-84, most others are the average of two tests.

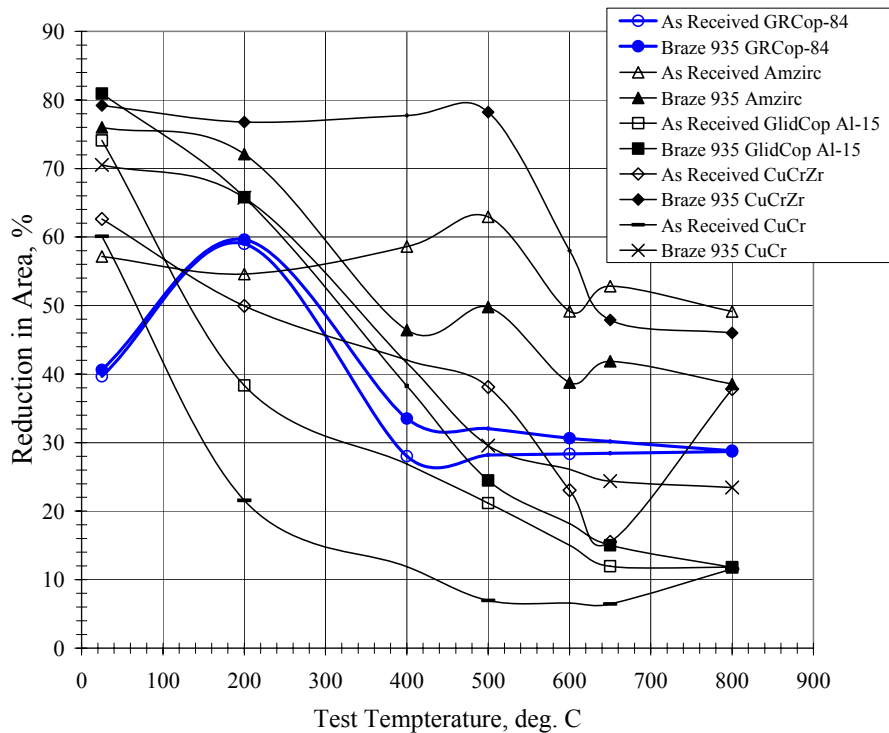


Figure 17. Reduction in cross-sectional area for as-received and brazed GRCop-84, AMZIRC, GlidCop Al-15, Cu-1Cr-0.1Zr, Cu-0.9Cr alloys. GRCop-84 values are the average of HIPed and extruded material, data points represent averages of multiple tests, five tests at each temperature for GRCop-84, most others are the average of two tests.

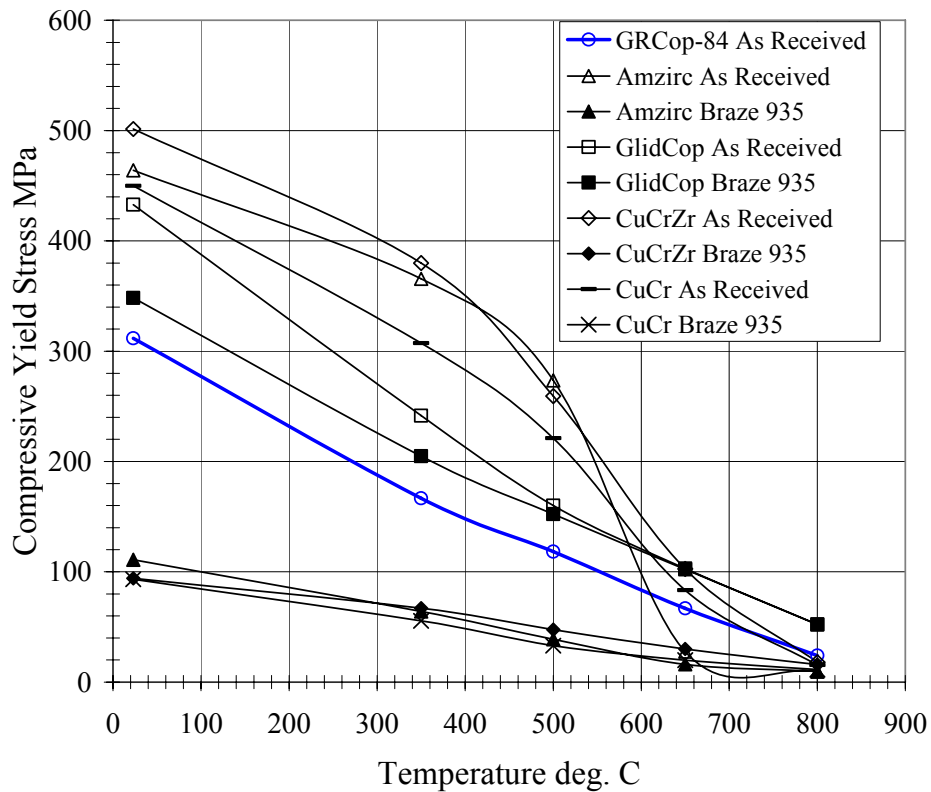
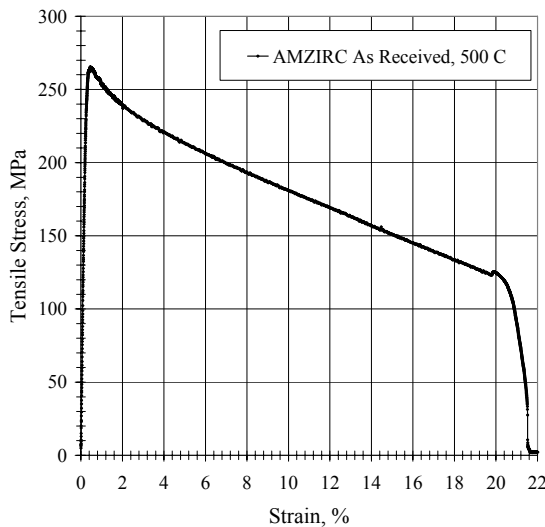
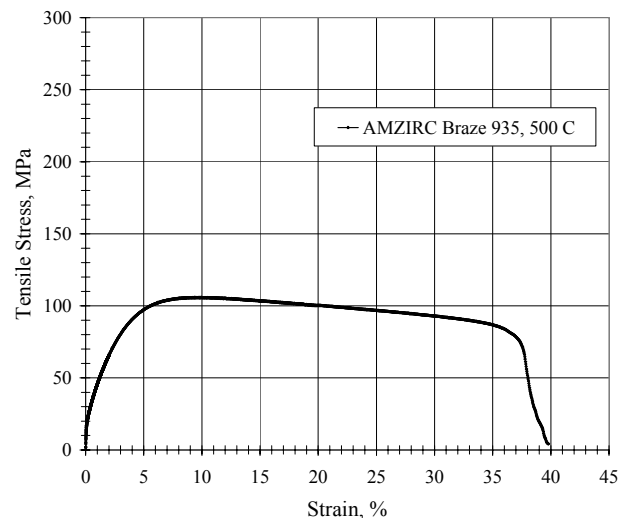


Figure 18. Compressive Yield Strength, defined as the compressive stress at 0.2% off-set strain, for GRCop-84, AMZIRC, GlidCop Al-15, Cu-1Cr-0.1Zr, and Cu-0.9Cr alloys at various test temperatures; data points are from averages of multiple tests, two or three tests at each temperature for each alloy.



a)



b)

Figure 19. Stress-strain curve in tension at 500 °C for a) as received AMZIRC and b) AMZIRC which has received the simulated brazing heat treatment; note the drop in ultimate stress and rise in peak strain compared to as received AMZIRC.

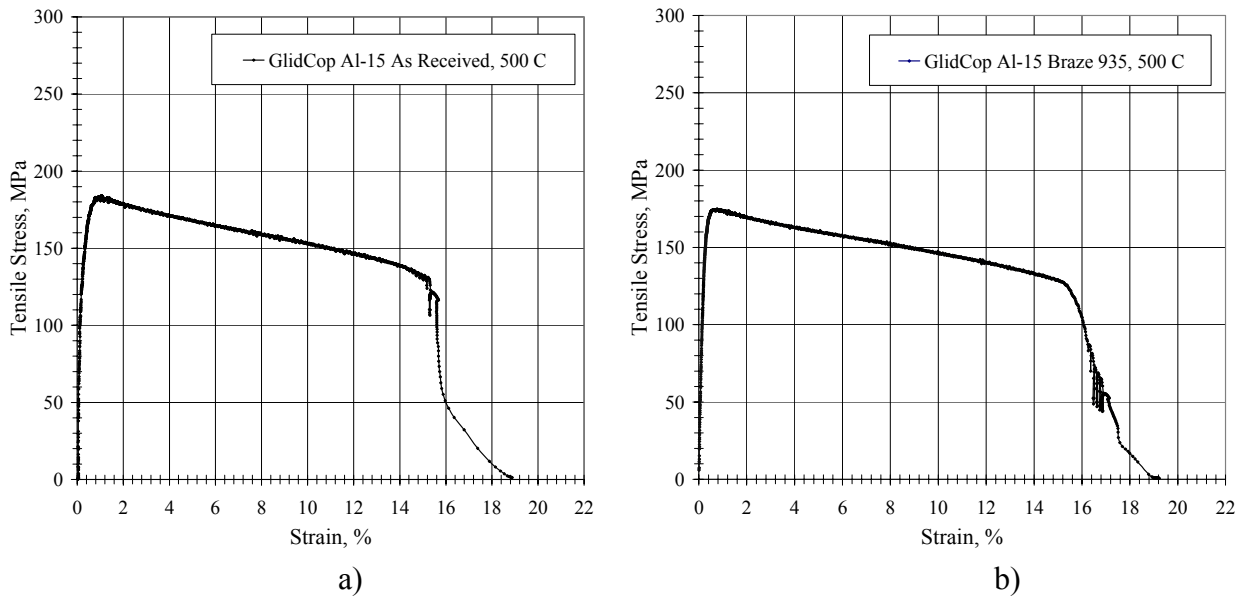


Figure 20. Stress-strain curve at 500 °C for GlidCop Al-15 in the a) as received condition, and b) after receiving the simulated braze heat treatment.

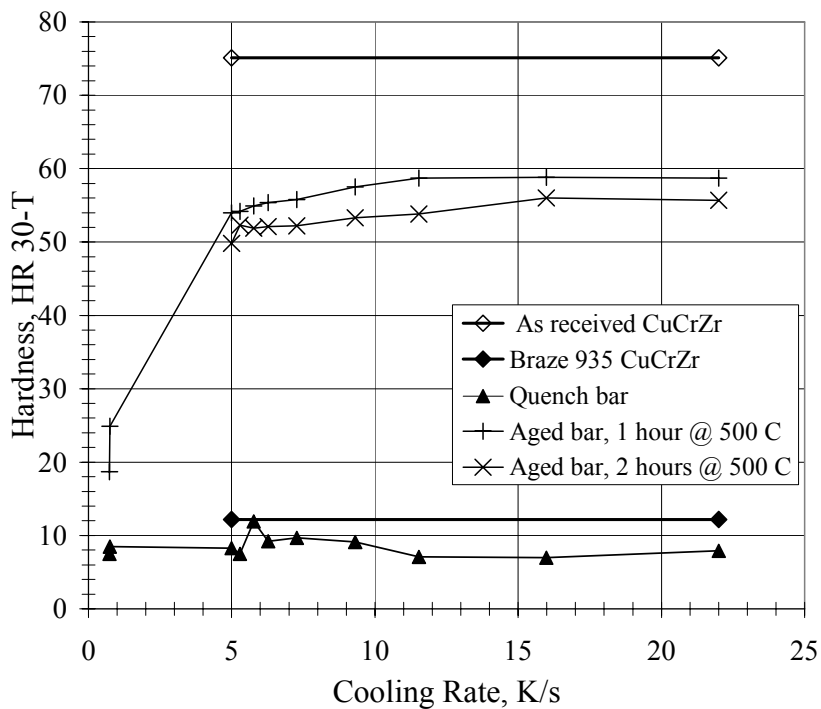


Figure 21. Hardness of a Cu-1Cr-0.1Zr bar after various treatments; cooling rate is the average cooling rate achieved during the quench from the solution temperature, 980 to 500 °C. As received and brazed conditions are shown for reference; Quenched bar is hardness after solution heat treatment at 980 °C and water quenching (cooling rates of >5 K/s) or air quenching (cooling rates <1 K/s).

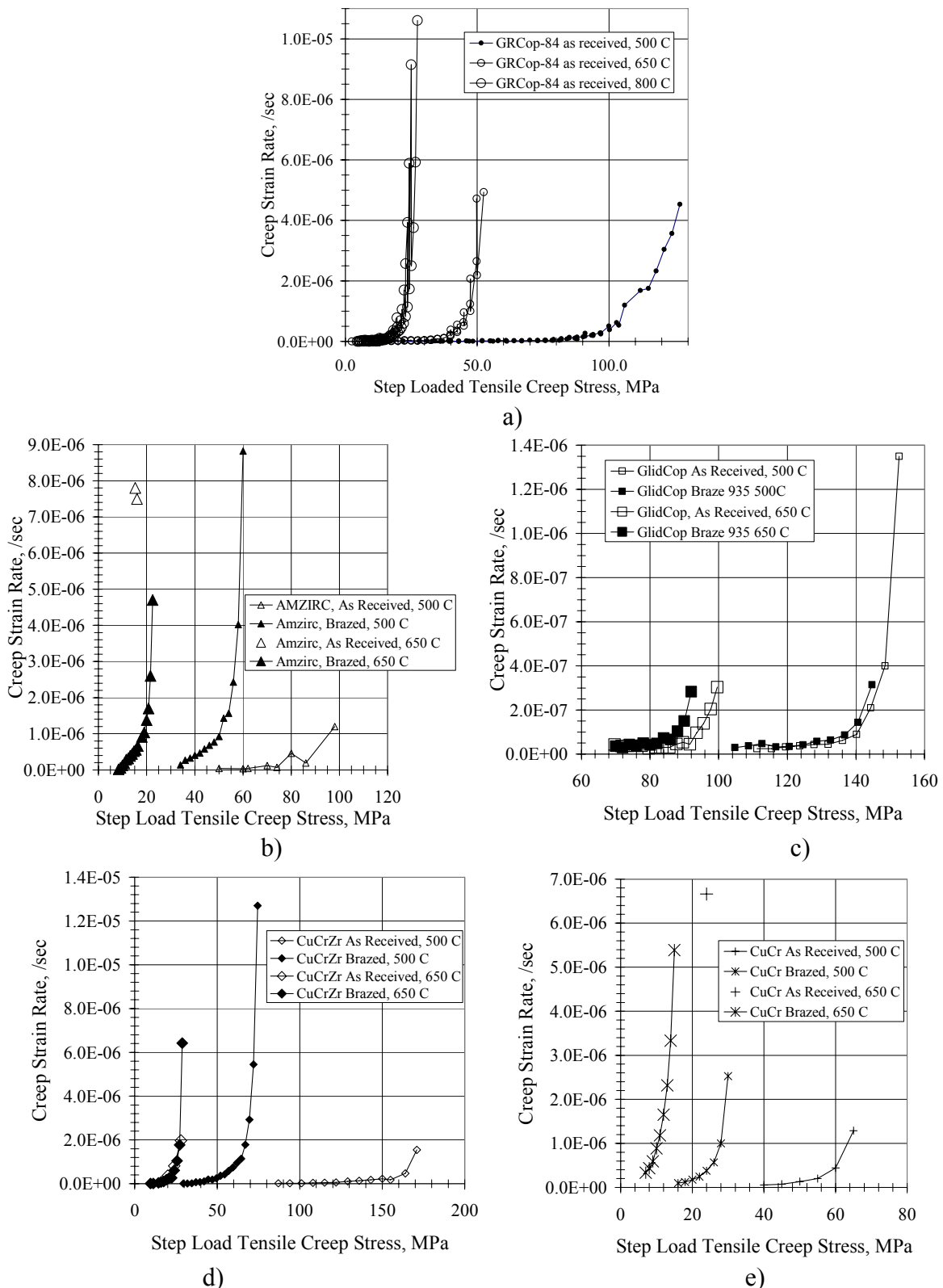


Figure 22. Steady state secondary creep strain rates during step loading at 500 and 650 °C of a) GRCop-84; b) AMZIRC; c) GlidCop Al-15; d) Cu-1Cr-0.1Zr; and e) Cu-0.9Cr. Small data point markers are at 500 °C, larger symbols are at 650 °C; open data markers are as received, filled data points have received the simulated braze heat treatment at 935 °C.

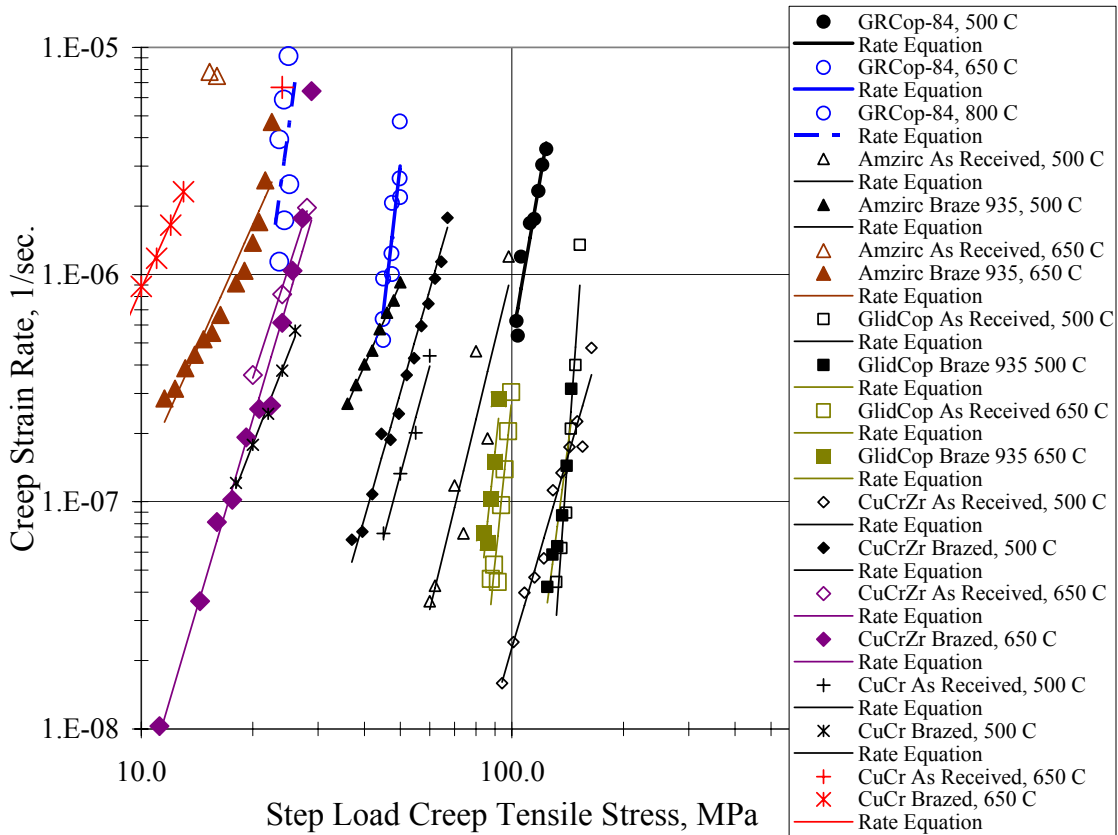
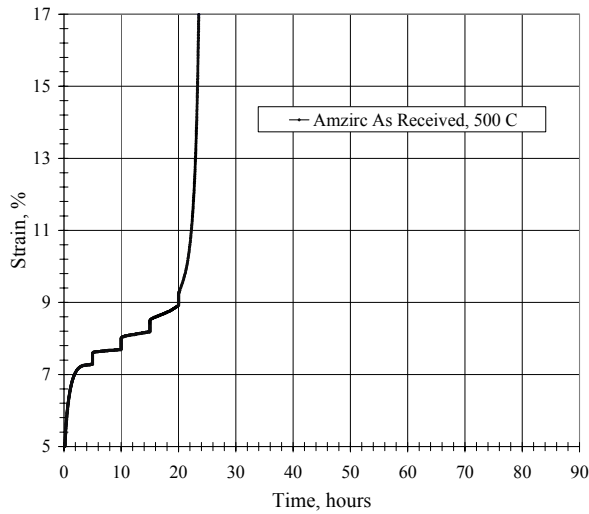
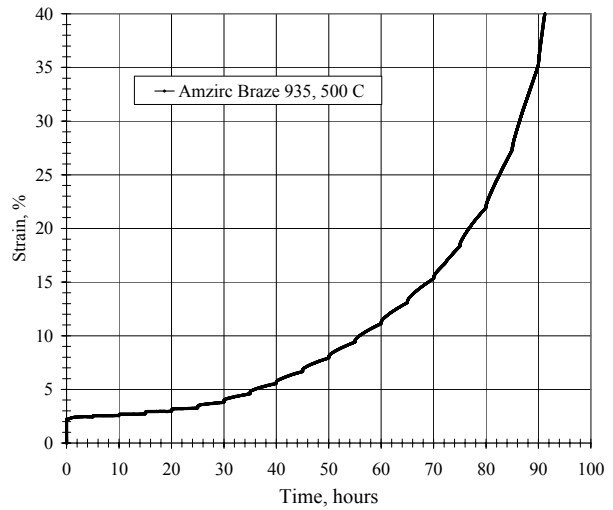


Figure 23. Step loaded creep rate data in the linear region of the log – log plot of strain rate and applied stress, with superimposed power function; power function constants are given in Table 9. All data at 500 °C are in black and use smaller symbols, data at 650 and 800 °C are gray (or color in the PDF version of this paper).

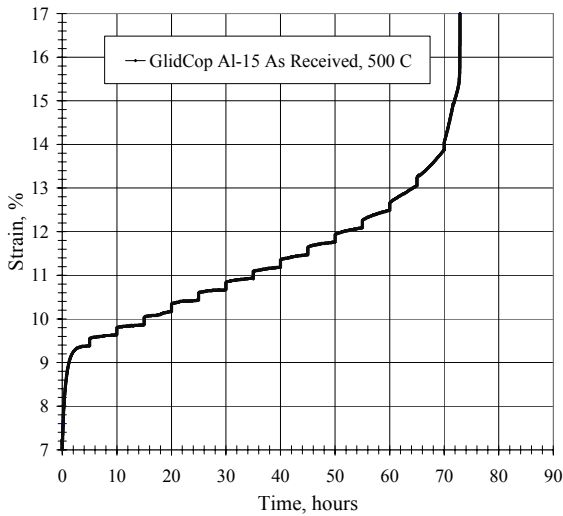


a)

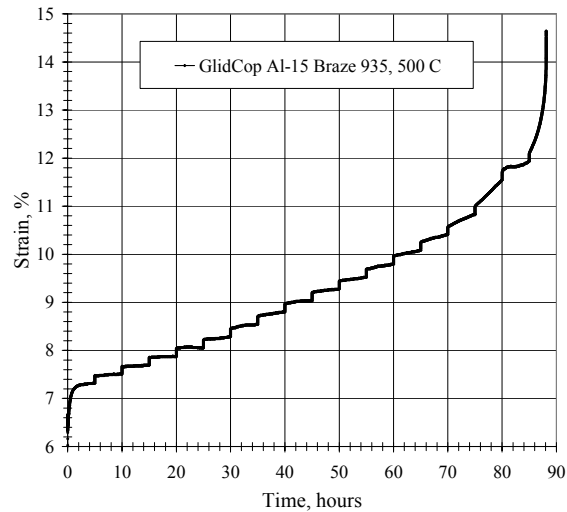


b)

Figure 24. Strain-Time data during step loaded creep at 500 °C for AMZIRC in the a) as received condition, and b) after receiving the simulated braze at 935 °C; the slopes of the steps are given in Table B6.



a)



b)

Figure 25. Step loaded creep strain in time at 500 °C for GlidCop Al-15 in the a) as received condition, and b) after the simulated braze at 935 °C; the slopes of the steps are given in Table B6.

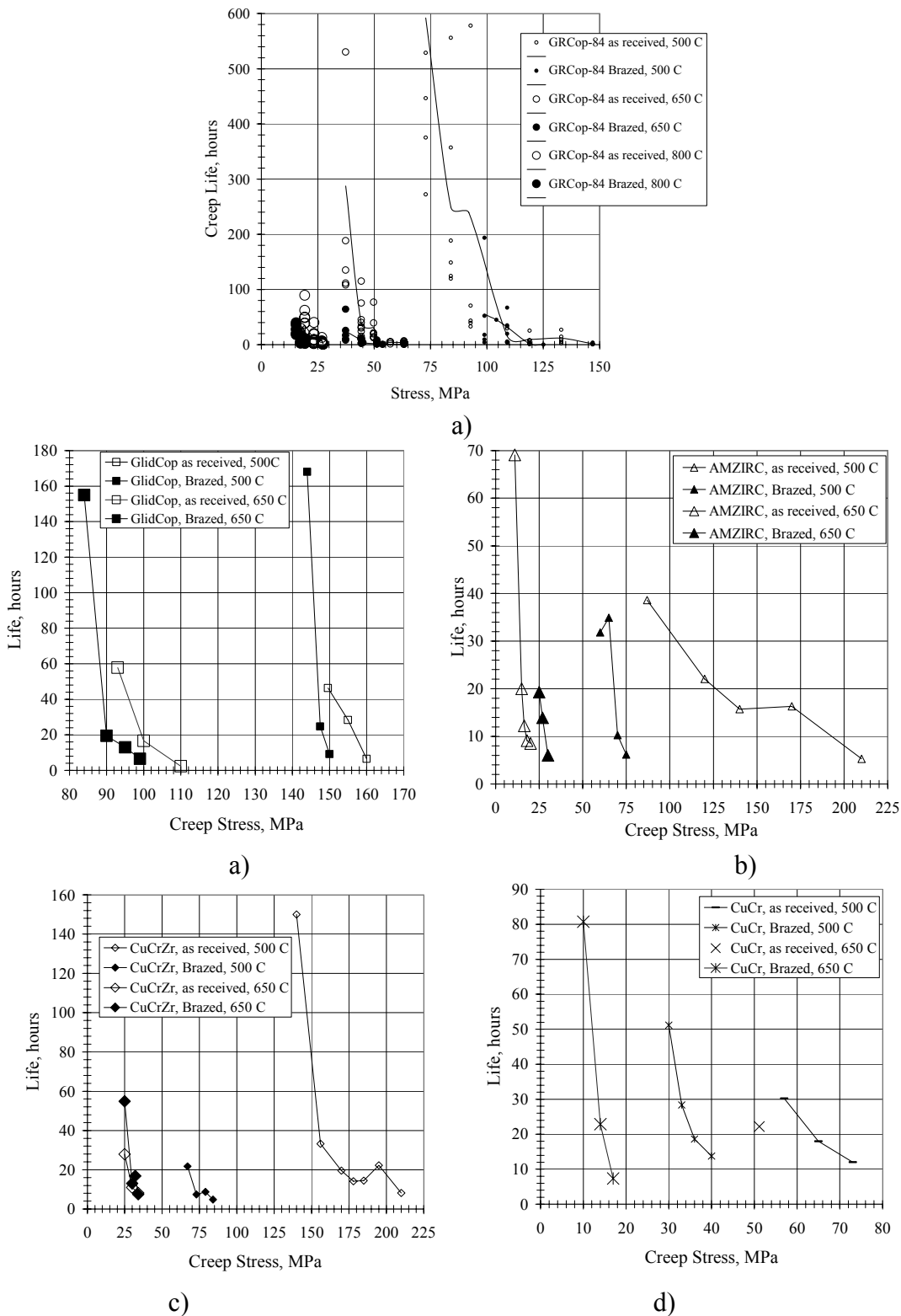


Figure 26. Time to failure during constant tensile load at 500 and 650 °C for a) GRCop-84; b) AMZIRC; c) GlidCop Al-15; d) Cu-1Cr-0.1Zr; and e) Cu-0.9Cr. Small data point markers are at 500 °C, larger symbols are at 650 °C; open data markers are as received, filled data points have had the simulated braze heat treatment at 935 °C. The lines in a) are through creep life averages at each stress.

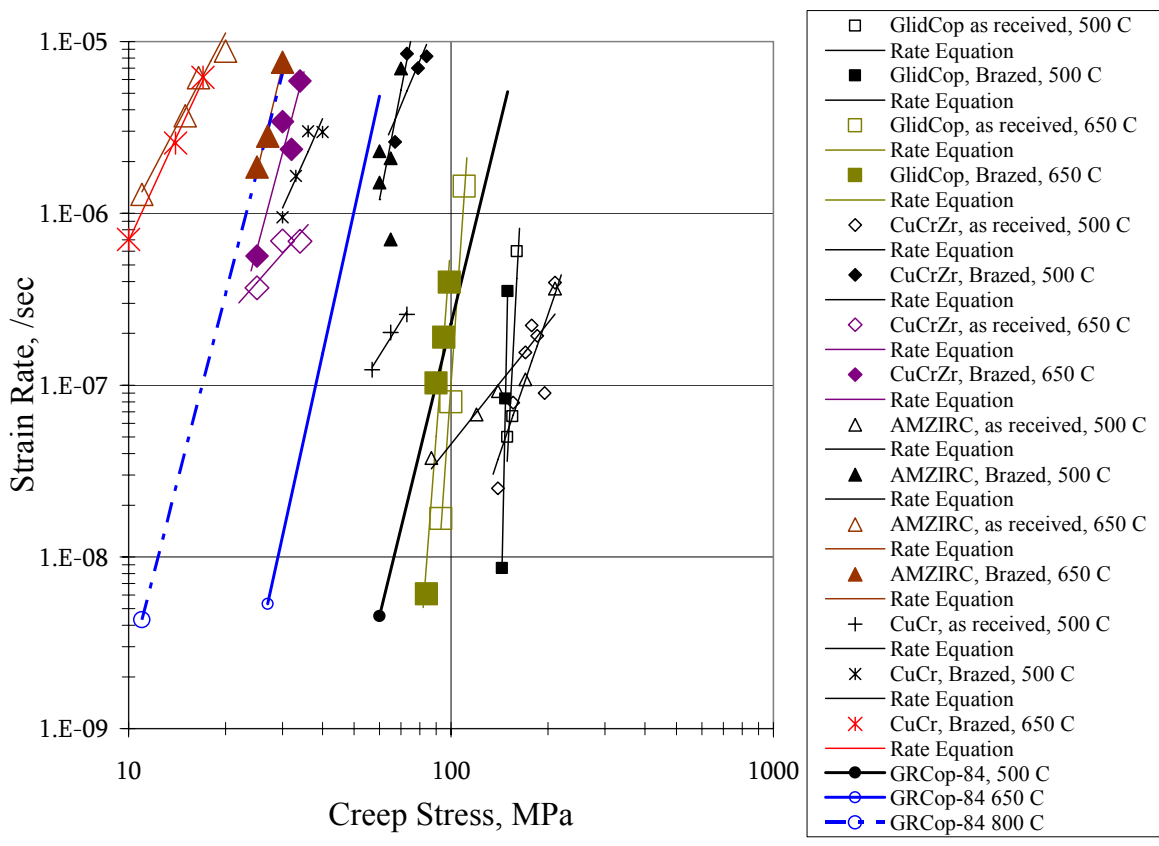


Figure 27. Constant load creep and resulting secondary creep strain rates with superimposed power law functions, power function constants shown in Table 11; data at 500 °C are black, larger like symbols are at the higher temperature. The GRCop-84 lines shown are from the power law creep rate equations presented in Table 11, from analysis of previous creep tests presented in Ref. 21.

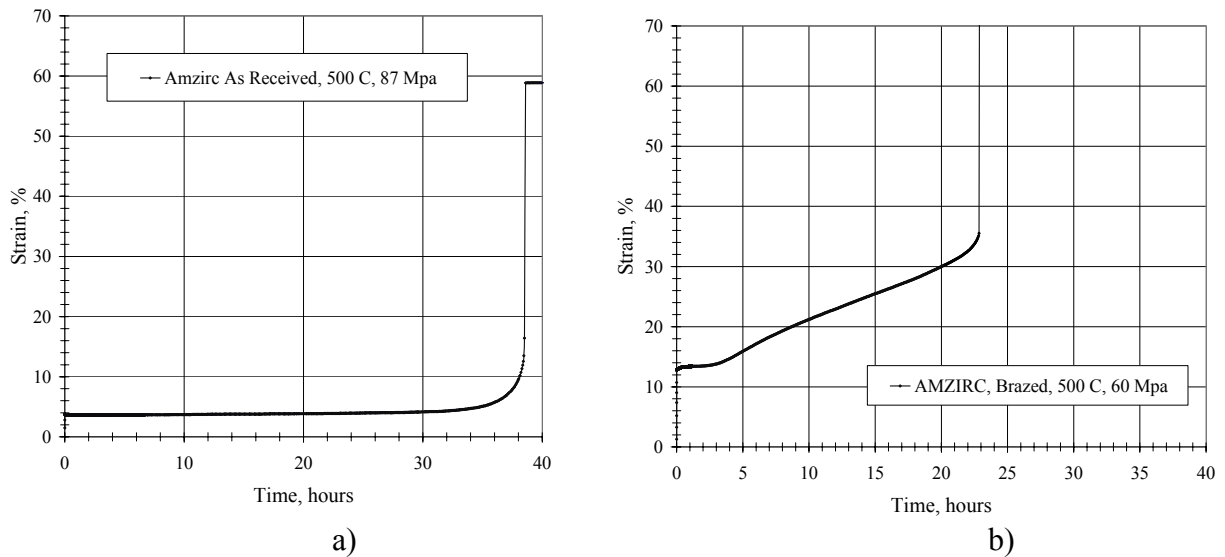


Figure 28. Constant load creep at 500 °C for AMZIRC in the a) as received condition, initial stress = 87 MPa, resulting in a creep rate of  $3.8 \times 10^{-8}$ /sec, and b) after the simulated braze, initial stress = 60 MPa, resulting in a creep rate of  $2.3 \times 10^{-6}$ /sec.



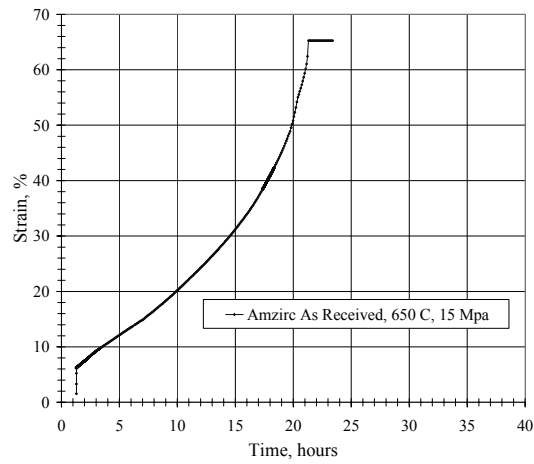


Figure 29. Constant load creep at 650 °C of as received Amzirc with initial stress = 15 MPa, resulting in a creep rate of  $3.7 \times 10^{-6}$ /sec.

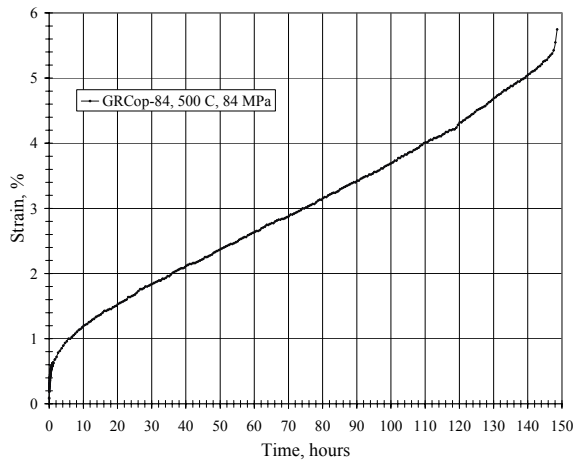


Figure 30. Constant load creep of GRCop-84 at 500 °C at an initial stress of 84 MPa, resulting in a creep rate of  $7.31 \times 10^{-8}$ /sec.

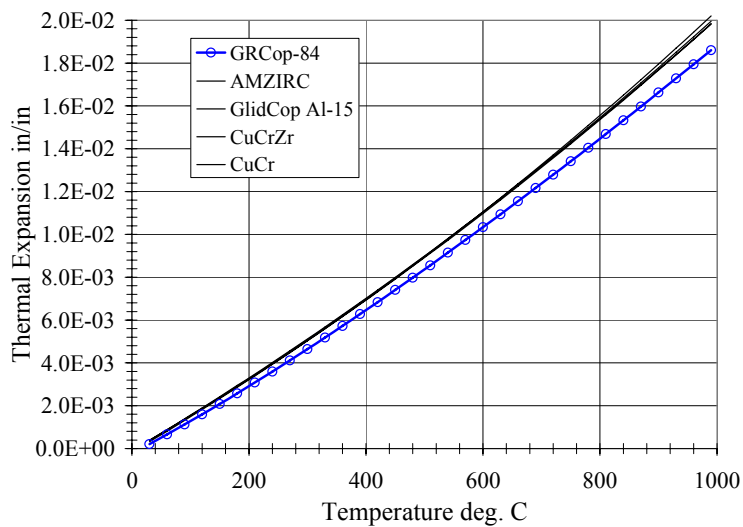


Figure 31. Thermal Expansion results, lines are plots of equation (1) and the quadratics from Table 12.

## References

- 1) Butler Jr., D.T., Pindera, M.J. "Analysis of Factors Affecting the Performance of RLV Thrust Cell Liners" NASA/CR-2004-213141, Aug. 2004.
- 2) Stephens, J.J., Schmale, D.T. "The effect of high temperature braze thermal cycles on mechanical properties of a dispersion strengthened copper alloy" SAND87-1296 • UC-20, 1987, 1988 second printing.
- 3) Nathal, M.V., Ellis, D.L., Loewenthal, W.S., Raj, S.V., Thomas-Ogbuji, L.U., Ghosn, J., Greenbauer-Seng, L.A., Gayda, J., Barrett, C.A., "High conductivity materials for high heat flux applications in space propulsion systems" JANNAF 39<sup>th</sup> CS/27<sup>th</sup> APS/21<sup>st</sup> PSHS/3<sup>rd</sup> MSS Subcommittee Joint Meeting, Colorado Springs, CO, CD-ROM, (Dec. 2003), p. 2003-0390cc.
- 4) Conway, J.B., Stentz, R.H., Berling, J.T. "High temperature, low cycle fatigue of copper-base alloys in argon; Part I – Preliminary results for 12 alloys at 1000 °F (538 °C)" NASA CR-121259, 1973.
- 5) Wycliffe, P.A., "Literature search on high conductivity copper based alloys" Final Report IDWA No. 6458-2, Rockwell International Sci. Center, R5739TC/sn, 1984.
- 6) Horn, D.D., Lewis, H.F., "Property Investigation of Copper Base Alloys at Ambient and Elevated Temperatures" AEDC-TR-65-72, 1965, (Defense Document Center No. 467015) p. 4, 11, 12, 35, 38.
- 7) Conway, J.B., Stentz, R.H., Berling, J.T., "High-Temperature, Low-Cycle Fatigue of Copper-Base Alloys for Rocket Nozzles, Part II – Strainrange Partitioning and Low-Cycle Fatigue Results at 538 °C" NASA CR-135073, 1976.
- 8) Hannum, N.P., Kasper, H.J., Pavli, A.J., "Experimental and Theoretical Investigation of Fatigue Life in Reusable Rocket Thrust Chambers" AIAA/SAE 12<sup>th</sup> Propulsion Conf., AIAA paper No. 76-685, 1976.
- 9) Esposito, J.J., Zabora, R.F. "Thrust Chamber Life Prediction – Vol. I – Mechanical and Physical Properties of High Performance Rocket Nozzle Materials" NASA CR-134806, 1975.
- 10) Dalder, E.N.C., Ludemann, W., Schumacher, B., "Thermal stability of four high-strength, high-conductivity copper sheet alloys" UCRL-88919, and ASM's Copper and Copper Alloys Conf., 1983, material also appears in UCRL-89034-Rev.1, Conf-830466-Rev-1, DE83 013312 Accession No. 84N10288, DOE Workshop on Copper Alloys, 1983.
- 11) Stephens, J.J., Bourcier, R.J., Vigil, F.J., Schmale, D.T., "Mechanical properties of dispersion strengthened copper: a comparison of braze cycle annealed and coarse grain microstructure" Sandia Report SAND88-1351 □UC-25, 1988.
- 12) Metals Handbook 9<sup>th</sup> Edition, Volume 2, Properties and Selection: Nonferrous Alloys and Pure Metals, ASM Handbook Committee, American Soc. for Metals, Metals Park, Ohio, p. 309.
- 13) Correia, J.B., Davies, H.A., Sellars, C.M., "Strengthening in rapidly solidified age hardened Cu-Cr and Cu-Cr-Zr alloys," Acta mater. Vol. 45, No. 1, pp. 177-190, 1997.
- 14) Zeng, K.J., Hamalainen, M., Lilius, K., "Phase relations in Cu-rich corner of the Cu-Cr-Zr phase diagram" Scripta Metallurgica et Materialia, Vol. 32, No. 12, 1995, pp. 2009-2014.
- 15) Pratt & Whitney Aircraft Group, "Thrust Chamber Material Technology Program" NASA-CR-187207, 1989.
- 16) Zinkle, S.J., "Tensile properties of high-strength, high-conductivity copper alloys at high temperatures," in Fusion Materials Semiann. Prog. Report for period ending June 30 2000,

- DOE/ER-0313/28, Oak Ridge National Lab, Oak Ridge, TN, 2000, pp. 171-175. Oak Ridge Nat. Lab. p. 171-175.
- 17) Chambers, A., personal communication, SpaceX, 2006.
- 18) Ellis, D.L., Dreshfield, R.L., “Preliminary evaluation of a powder metal copper-8 Cr-4 Nb alloy” in *Advanced Earth-to-Orbit Propulsion Technology 1992*, NASA CP-3174, Vol. 1., NASA MSFC, Huntsville AL, May 1992, p. 18-27.
- 19) Ellis, D.L., Dreshfield, R.L., Verrilli, M.J., Ulmer, D.G. “Mechanical Properties of a Cu-8 Cr-4 Nb alloy” in *Advanced Earth-to-Orbit Propulsion Technology 1994*, NASA CP-3282, NASA MSFC, Huntsville AL, May. 1994, p. 32-41.
- 20) Ellis, D.L., Michal, G.M., “Mechanical and thermal properties of two Cr-Cr-Nb alloys and NARloy-Z” NASA CR 198529, NASA Glenn Research Center, Cleveland OH, Oct. 1996.
- 21) David L. Ellis, William S. Loewenthal and Harold Haller, “Creep of Commercially Produced GRCop-84,” NASA TM to be published, NASA GRC, Cleveland, OH (2006)
- 22) Goldsmith, A., Waterman, T.E., Hirschhorn, H.J.: Handbook of Thermophysical Properties of Solid Materials, Vol. 1, Pergamon, New York, NY 1961.
- 23) Wilson, Mechanical Instrument Div., Wilson Pocket Relationship Table 52, Wilson Cylindrical Correction Chart #53, 1953.
- 24) D. L. Ellis and G. M. Michal, Formation of Cr and Cr<sub>2</sub>Nb precipitates in rapidly solidified Cu-Cr-Nb ribbon, *Ultramicroscopy*, Volume 30, Issues 1-2, , June 1989, p. 210-216. <http://www.sciencedirect.com/science/article/B6TW1-46MKWY1-7D/2/d7c1dea1aa45d184ef0b455b19f285df>
- 25) Verhoeven J.D., Fundamentals of Physical Metallurgy, John Wiley & Sons pub., 1975, p. 330, 459, 515-517.
- 26) ASM Handbook, Vol. 8, Mechanical Testing and Evaluation, Kuhn, H., Medlin, D. editors, ASM International, 2000, p. 363-368.
- 27) Ellis, D.L., Keller, D.J., “Thermophysical Properties of GRCop-84”, NASA/CR-2000-210055, NASA GRC, Cleveland, OH (June 2000).

# REPORT DOCUMENTATION PAGE

*Form Approved*  
*OMB No. 0704-0188*

Public reporting burden for this collection of information is estimated to average 1 hour per response, including the time for reviewing instructions, searching existing data sources, gathering and maintaining the data needed, and completing and reviewing the collection of information. Send comments regarding this burden estimate or any other aspect of this collection of information, including suggestions for reducing this burden, to Washington Headquarters Services, Directorate for Information Operations and Reports, 1215 Jefferson Davis Highway, Suite 1204, Arlington, VA 22202-4302, and to the Office of Management and Budget, Paperwork Reduction Project (0704-0188), Washington, DC 20503.

<b>1. AGENCY USE ONLY</b> ( <i>Leave blank</i> )	<b>2. REPORT DATE</b> February 2007	<b>3. REPORT TYPE AND DATES COVERED</b> Technical Memorandum	
<b>4. TITLE AND SUBTITLE</b>  Comparison of GRCop-84 to Other High Thermal Conductive Cu Alloys		<b>5. FUNDING NUMBERS</b>  WBS 599489.02.07.03.02.04.01	
<b>6. AUTHOR(S)</b>  Henry C. de Groh III, David L. Ellis, and William S. Loewenthal			
<b>7. PERFORMING ORGANIZATION NAME(S) AND ADDRESS(ES)</b>  National Aeronautics and Space Administration John H. Glenn Research Center at Lewis Field Cleveland, Ohio 44135-3191		<b>8. PERFORMING ORGANIZATION REPORT NUMBER</b>  E-15798	
<b>9. SPONSORING/MONITORING AGENCY NAME(S) AND ADDRESS(ES)</b>  National Aeronautics and Space Administration Washington, DC 20546-0001		<b>10. SPONSORING/MONITORING AGENCY REPORT NUMBER</b>  NASA TM-2007-214663	
<b>11. SUPPLEMENTARY NOTES</b>  Henry C. de Groh III and David L. Ellis, NASA Glenn Research Center, Cleveland, Ohio; and William S. Loewenthal, Ohio Aerospace Institute, 28000 Cedar Point Road, Brook Park, Ohio 44142. Responsible person, Henry C. de Groh III, organization code RXA, 216-433-5025.			
<b>12a. DISTRIBUTION/AVAILABILITY STATEMENT</b>  Unclassified - Unlimited Subject Categories: 20 and 26  Available electronically at <a href="http://gltrs.grc.nasa.gov">http://gltrs.grc.nasa.gov</a>  This publication is available from the NASA Center for AeroSpace Information, 301-621-0390.		<b>12b. DISTRIBUTION CODE</b>	
<b>13. ABSTRACT</b> ( <i>Maximum 200 words</i> )  The mechanical properties of five copper alloys (GRCop-84, AMZIRC, GlidCop Al-15, Cu-1Cr-0.1Zr, Cu-0.9Cr) competing in high temperature, high heat flux applications such as rocket nozzles, were compared. Tensile, creep, thermal expansion, and compression tests are presented. Tests were done on as-received material, and on material which received a simulated brazing heat treatment at 935 °C. The 935 °C heat treatment weakened AMZIRC, Cu-1Cr-0.1Zr, and Cu-0.9Cr, and the strength of as-received AMZIRC dropped precipitously as test temperatures exceeded 500 °C. The properties of GlidCop Al-15 and GRCop-84 were not significantly affected by the 935 °C heat treatment. Thus GRCop-84 is better than AMZIRC, Cu-1Cr-0.1Zr, and Cu-0.9Cr at temperatures greater than 500 °C. Ductility was lowest in GlidCop Al-15 and Cu-0.9Cr. The creep properties of GRCop-84 were superior to those of brazed AMZIRC, Cu-1Cr-0.1Zr, and Cu-0.9Cr. At equivalent rupture life and stress, GRCop-84 had a 150 °C temperature advantage over brazed AMZIRC; for equivalent rupture life and temperature GRCop-84 was two times stronger. The advantages of GRCop-84 over GlidCop Al-15 associated with ease of processing were confirmed by GlidCop's marginal ductility. In the post brazed condition, GRCop-84 was found to be superior to the other alloys due to its greater strength and creep resistance (compared to AMZIRC, Cu-1Cr-0.1Zr, and Cu-0.9Cr) and ductility (compared to GlidCop Al-15).			
<b>14. SUBJECT TERMS</b>  GRCop-84; AMZIRC; GlidCop Al-15; Cu-Cr-Zr; Cu-Cr; Copper: Compression; Tension; Creep; Mechanical properties		<b>15. NUMBER OF PAGES</b> 53	
		<b>16. PRICE CODE</b>	
<b>17. SECURITY CLASSIFICATION OF REPORT</b> Unclassified	<b>18. SECURITY CLASSIFICATION OF THIS PAGE</b> Unclassified	<b>19. SECURITY CLASSIFICATION OF ABSTRACT</b> Unclassified	<b>20. LIMITATION OF ABSTRACT</b>



